KITP
Feb.2012

Sounds of the Little Bang thermalization and jet quenching

Edward Shuryak

Department of Physics and Astronomy

Stony Brook

Plan

- The Little Bang comes to LHC
- Sound in Big and Little Bang: The second act of hydro **(all harmonics)**
- The falling membrane: 1-point local vs 2-point (nonlocal) observables: the echo effect
- LHC jet quenching in AdS
- Quenching due to the **gravitational radiation** in BH AdS: What is its dependence on jet energy? Is it equal to the ``self-force''?

on hydrodynamics

- Field theory development was helped by hydro in the 19th century (PDEs, Stokes-> Maxwell…)
- Fermi…Landau in 1950's: Landau pole argument
- But when I was dreaming about it in 1970's most theorists said it is ridiculously simplistic to describe anything and that it obviously contradicts both quantum mechanics and QCD
- Not anymore: now, using AdS/CFT correspondence, one derives it from the **membrane paradigm of GR**
- (Hydro has dissipation/equilibration and Einstein's eqns are t-even: how can it be true? Well, boundary conditions on the black hole horizon are NOT, as everything falls into it but nothing comes out…)

Back to QM1999: hydro vs pQCD

Elliptic flow

How does the system respond to initial spatial anisotropy?

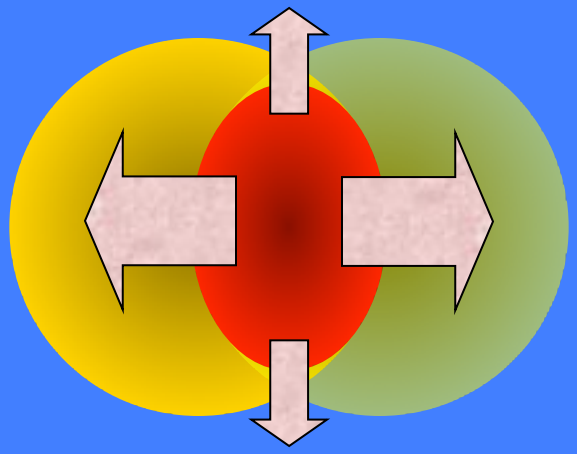

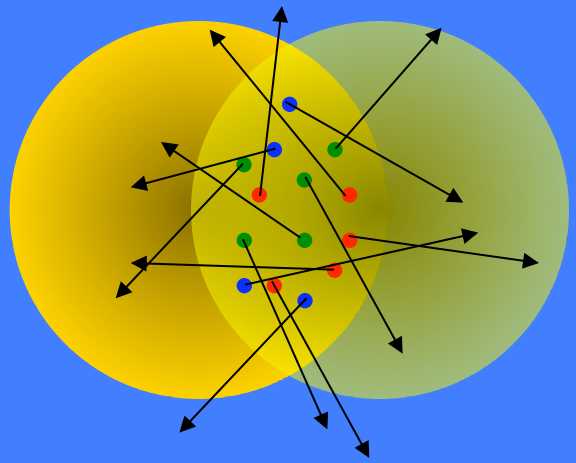

$$\frac{dN}{p_T dp_T dy d\phi} = \frac{1}{2\pi}\frac{dN}{p_T dp_T dy}(1 + 2v_1\cos(\phi) + 2v_2\cos(2\phi) + \cdots)$$

$$v_2(p_T, y) = \frac{\int d\phi \cos(2\phi)\frac{dN}{p_T dp_T dy d\phi}}{\int d\phi \frac{dN}{p_T dp_T dy d\phi}} = \langle\cos(2\phi)\rangle$$

2000: hydro describes radial and elliptic flows for all secondaries , pt<2GeV, centralities, rapidities, A (Cu,Au)…
Experimentalists were very sceptical but were convinced and ``near-perfect liquid" is now official,

=>AIP declared this to be discovery #1 of 2005 in physics

v_2≡<cos(2 phi)>

proton **pion**

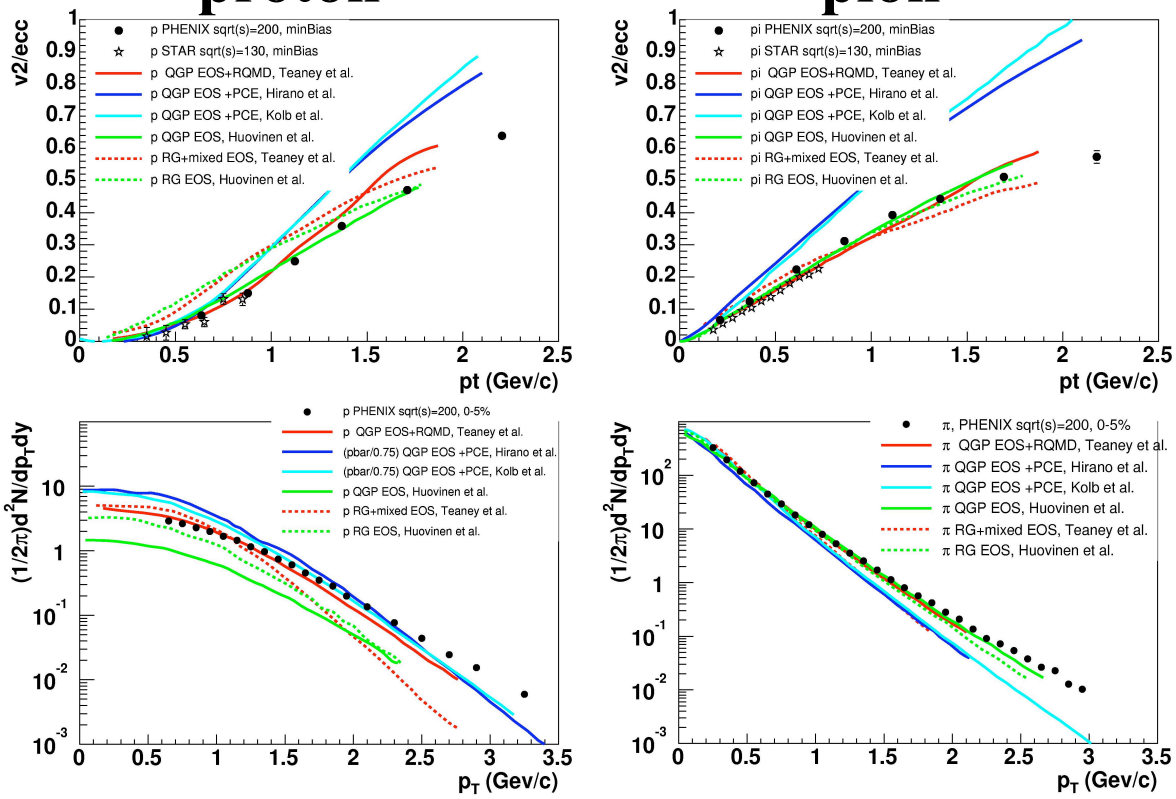

PHENIX,
Nucl-ex/0410003

red lines are for ES +Lauret+Teaney done before RHIC data, never changed or fitted, describes SPS data as well! It does so because of the correct hadronic matter /freezout via (RQMD)

While our experimental friends had made their detectors, the theorists debated

Will it be like that at LHC?

- Energy is up by about factor 20
- Initial T changes from 2Tc -> 3 Tc

(Tc about 170 MeV)

- Multiplicity is up by 2.2
- Will QGP change from strongly to weakly coupled regime?**=>will v2 go up or down?**

Viewpoint

A "Little Bang" arrives at the LHC

Edward Shuryak
Department of Physics and Astronomy, Stony Brook University, Stony Brook, NY 11794, USA
Published December 13, 2010

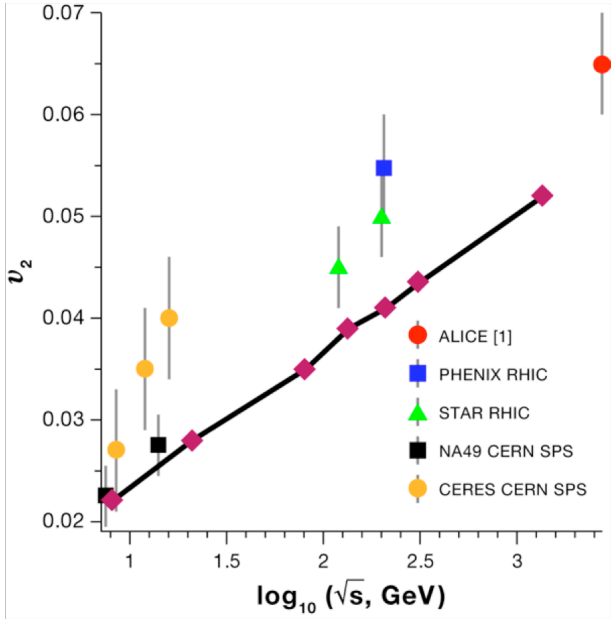

FIG. 1: The ALICE experiment suggests that the quark-gluon plasma remains a strongly coupled liquid, even at temperatures that are 30% greater than what was available at RHIC. The plot shows the "elliptic flow parameter" v_2 (a measure of the coupling in the plasma) at different heavy-ion collision energies, based on several experiments (including the new data from ALICE [1]). (Note the energy scale is plotted on a logarithmic scale and spans three orders of magnitude.) The trend is consistent with theoretical predictions (pink diamonds) for an ideal liquid [4].

Increased elliptic and radial flows, as well as increased HBT radii/volume are all supporting "Hydro1", the "Little Bang"

What do these results tell us about the quark-gluon plasma? The mean free path for particles in the plasma can be conveniently expressed via a dimensionless ratio $(\eta/s\hbar)$, where η is the shear viscosity, s is the entropy density and $\hbar$ is Planck's constant. In a weakly coupled quark-gluon plasma, the mean free path should be large $(\eta/s\hbar \gg 1)$, while it should be small in a strongly coupled plasma. RHIC data analysis has shown it to be extremely small, close to the theoretically conjectured lower limit $\eta/s\hbar = 1/4\pi$ for infinitely strong coupling [5]. That this strong-coupling picture holds for the QGP seen at the LHC seems now likely. Naively, one might

Perturbations of the Big Bang

Perturbations of the Big and the Little Bangs

Frozen sound (from the era long gone) is seen on the sky, both in CMB and in distribution of Galaxies

$$\frac{\Delta T}{T} \sim 10^{-5}$$

$$l_{maximum} \approx 210$$

$$\delta\phi \sim 2\pi/l_{maximum} \sim 1^o$$

They are remnants of the sound circles on the sky, around the primordial density perturbations
Freezeout time 100000 years

Initial state fluctuations
in the positions of participant nucleons
lead to perturbations of the Little Bang also

$$\frac{\Delta T}{T} \sim 10^{-2}$$

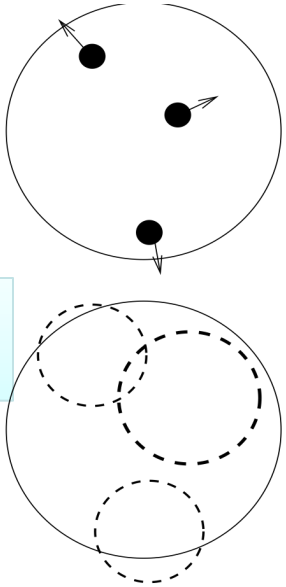

Freezeout time about 12 fm/c
Radius of the circle about 6 fm

PHYSICAL REVIEW C **80**, 054908 (2009)

Fate of the initial state perturbations in heavy ion collisions

Edward Shuryak
Department of Physics and Astronomy, State University of New York, Stony Brook, New York 11794, USA
(Received 20 July 2009; revised manuscript received 14 October 2009; published 13 November 2009)

ACOUSTIC SIGNATURES IN THE COSMIC MICROWAVE BACKGROUND

Wayne Hu
Institute for Advanced Study
School of Natural Sciences
Princeton, NJ 08540

and

Martin White
Enrico Fermi Institute
University of Chicago
Chicago, IL 60637

ABSTRACT

We study the uniqueness and robustness of acoustic signatures in the cosmic microwave background by allowing for the possibility that they are generated by some as yet unknown source of gravitational perturbations. The acoustic *pattern* of peak locations and relative heights predicted by the standard inflationary cold dark matter model is essentially unique and its confirmation would have deep implications for the causal structure of the early universe. A generic pattern for isocurvature initial conditions arises due to backreaction effects but is not robust to exotic source behavior inside the horizon. If present, the acoustic pattern contains unambiguous information on the curvature of the universe even in the general case. By classifying the behavior of the unknown source, we determine the minimal observations necessary for robust constraints on the curvature. The diffusion damping scale provides an entirely model independent cornerstone upon which to build such a measurement. The peak spacing, if regular, supplies a precision test.

Subject headings: cosmology:theory – cosmic microwave background

Acoustic peaks

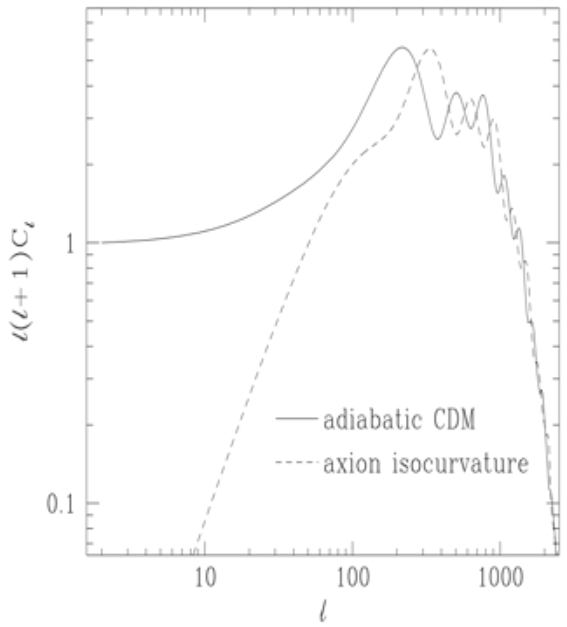

Dissipative cutoff

Fig. 6.— Diffusion damping.

Although adiabatic and isocurvature models predict acoustic oscillations in different positions, they both suffer diffusion damping in the same way. The damping length is fixed by background assumptions, here $\Omega_0 = 1$, $h = 0.5$, $\Omega_b = 0.05$ and standard recombination. These calculations were performed using a full numerical integration of the Boltzmann equation with the code of Sugiyama (1995) as were results in Figs. 7,8,10,11.

Seven-Year Wilkinson Microwave Anisotropy Probe (WMAP[1]) Observations: Sky Maps, Systematic Errors, and Basic Results

N. Jarosik[2], C. L. Bennett[3], J. Dunkley[4], B. Gold[3], M. R. Greason[5], M. Halpern[6], R. S. Hill[5], G. Hinshaw[7], A. Kogut[7], E. Komatsu[8], D. Larson[3], M. Limon[9], S. S. Meyer[10], M. R. Nolta[11], N. Odegard[5], L. Page[2], K. M. Smith[12], D. N. Spergel[12,13], G. S. Tucker[14], J. L. Weiland[5], E. Wollack[7], E. L. Wright[15]

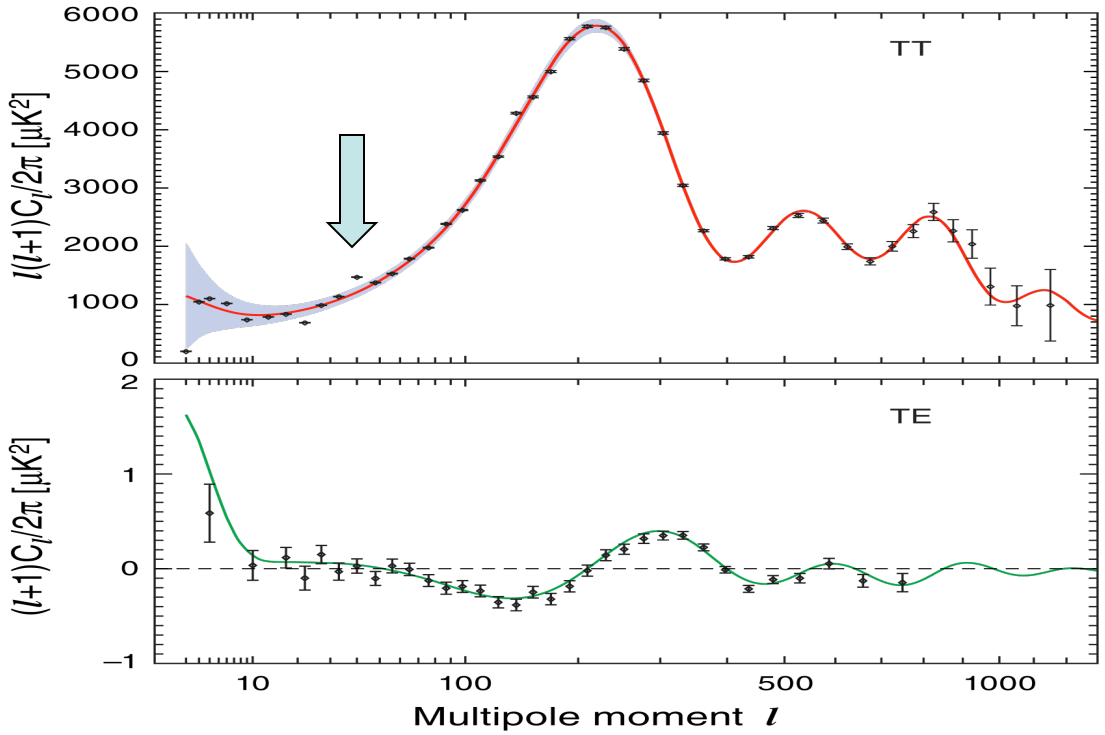

Fig. 9.— The temperature (TT) and temperature-polarization(TE) power spectra for the seven-year *WMAP* data set. The solid lines show the predicted spectrum for the best-fit flat ΛCDM model. The error bars on the data points represent measurement errors while the shaded region indicates the uncertainty in the model spectrum arising from cosmic variance. The model parameters are: $\Omega_b h^2 = 0.02260 \pm 0.00053$, $\Omega_c h^2 = 0.1123 \pm 0.0035$, $\Omega_\Lambda = 0.728^{+0.015}_{-0.016}$, $n_s = 0.963 \pm 0.012$, $\tau = 0.087 \pm 0.014$ and $\sigma_8 = 0.809 \pm 0.024$.

Unexplained Phenomena at small harmonics

The new space mission, PLANK, will provide much better data in 2012

DETECTION OF THE BARYON ACOUSTIC PEAK IN THE LARGE-SCALE CORRELATION FUNCTION OF SDSS LUMINOUS RED GALAXIES

Daniel J. Eisenstein[1,2], Idit Zehavi[1], David W. Hogg[3], Roman Scoccimarro[3], Michael R. Blanton[3], Robert C. Nichol[4], Ryan Scranton[5], Hee-Jong Seo[1], Max Tegmark[6,7], Zheng Zheng[8], Scott F. Anderson[9], Jim Annis[10], Neta Bahcall[11], Jon Brinkmann[12], Scott Burles[7], Francisco J. Castander[13], Andrew Connolly[5], Istvan Csabai[14], Mamoru Doi[15], Masataka Fukugita[16], Joshua A. Frieman[10,17], Karl Glazebrook[18], James E. Gunn[11], John S. Hendry[10], Gregory Hennessy[19], Zeljko Ivezić[9], Stephen Kent[10], Gillian R. Knapp[11], Huan Lin[10], Yeong-Shang Loh[20], Robert H. Lupton[11], Bruce Margon[21], Timothy A. McKay[22], Avery Meiksin[23], Jeffery A. Munn[19], Adrian Pope[18], Michael W. Richmond[24], David Schlegel[25], Donald P. Schneider[26], Kazuhiro Shimasaku[27], Christopher Stoughton[10], Michael A. Strauss[11], Mark SubbaRao[17,28], Alexander S. Szalay[18], István Szapudi[29], Douglas L. Tucker[10], Brian Yanny[10], & Donald G. York[17]

Submitted to The Astrophysical Journal 12/31/2004

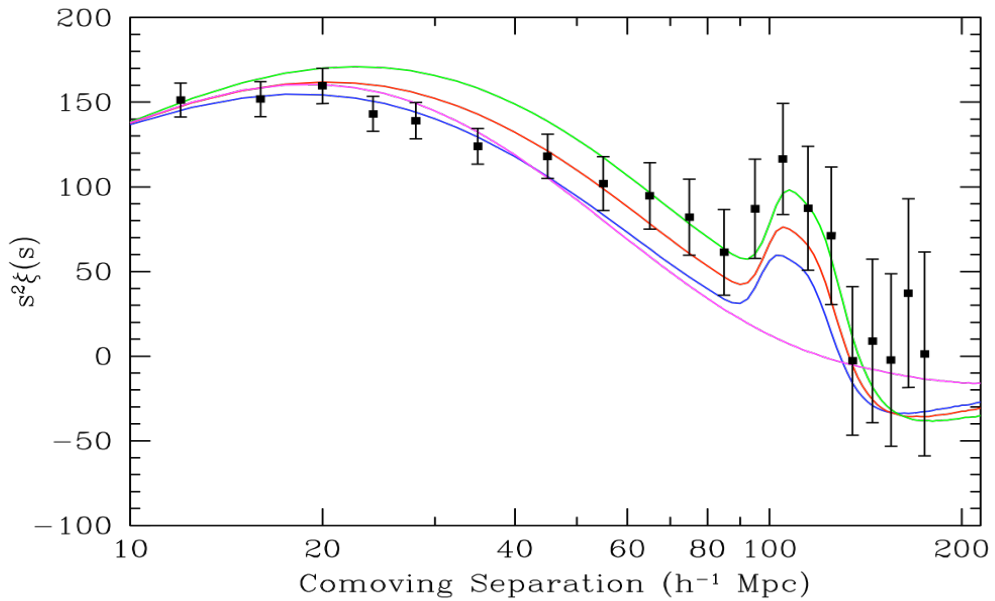

FIG. 3.— As Figure 2, but plotting the correlation function times s^2. This shows the variation of the peak at $20h^{-1}$ Mpc scales that is controlled by the redshift of equality (and hence by $\Omega_m h^2$). Varying $\Omega_m h^2$ alters the amount of large-to-small scale correlation, but boosting the large-scale correlations too much causes an inconsistency at $30h^{-1}$ Mpc. The pure CDM model (magenta) is actually close to the best-fit due to the data points on intermediate scales.

Back to the Little Bang

Two fundamental scales, describing perturbations **at freezeout**

(P.Staig,ES,2010)

1. The sound horizon: radius of about 6fm

$$H_s = \int_0^{\tau_f} d\tau c_s(\tau)$$

For the Big Bang it was introduced by Sunyaev-Zeldovich about 40 years ago, was observed in CMB and galaxy correlations, it is about 150 Mps

2. The viscous horizon: The width of the circle

$$\delta T_{\mu\nu}(t) = exp\left(-\frac{2}{3}\frac{\eta}{s}\frac{k^2 t}{3T}\right)\delta T_{\mu\nu}(0)$$

$$k_v = \frac{2\pi}{R_v} = \sqrt{\frac{3Ts}{2\tau_f \eta}} \sim 200 MeV$$

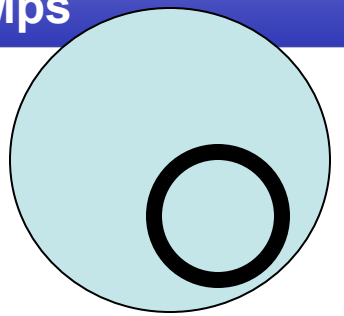

cylinders

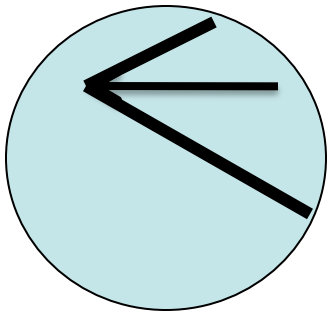

cones

Perturbations of the Big and the Little Bangs

Frozen sound (from the era long gone) is seen on the sky, both in CMB and in distribution of Galaxies

$$\frac{\Delta T}{T} \sim 10^{-5}$$

$$l_{maximum} \approx 210$$

$$\delta\phi \sim 2\pi/l_{maximum} \sim 1^o$$

They are literally circles on the sky, around primordial density perturbations

Initial state fluctuations
in the positions of participant nucleons
lead to perturbations of the Little Bang also

$$\frac{\Delta T}{T} \sim 10^{-2}$$

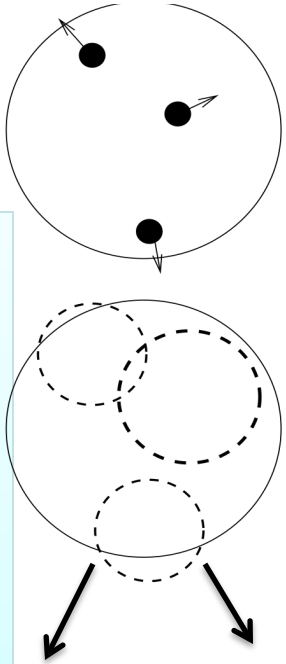

Blue shifting: exp(-u_i p_i/T)

Radial flow enhances the fireball surface: move toward detection with v about 0.8 c
So we should see two "horns"

The circle is that of maximal radial flow

Visible shape of the sound (at freezeout, boosted by radial flow)

PHYSICAL REVIEW C **80**, 054908 (2009)

Fate of the initial state perturbations in heavy ion collisions

Edward Shuryak
Department of Physics and Astronomy, State University of New York, Stony Brook, New York 11794, USA
(Received 20 July 2009; revised manuscript received 14 October 2009; published 13 November 2009)

Peak at +- 1 rad, 60°?

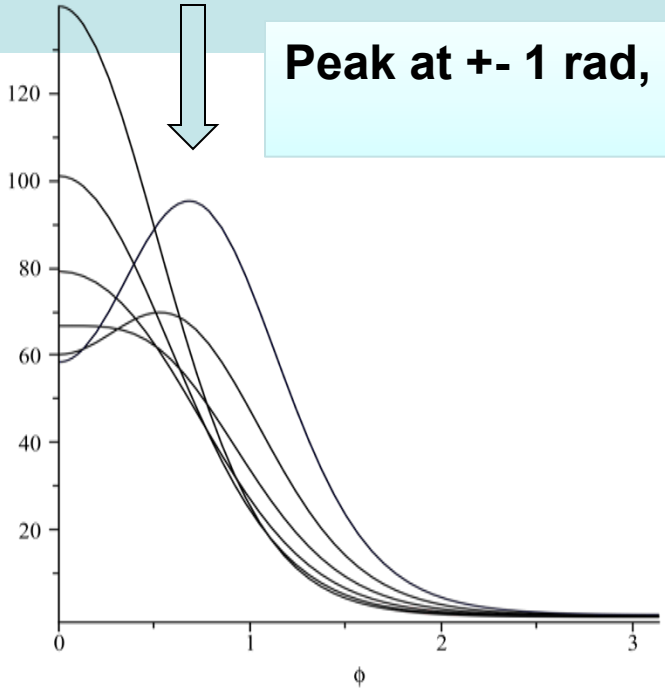

FIG. 5. (Color online) Dependence of the visible distribution in the azimuthal angle on the width of the (semi)circle at the time of freeze-out. Six curves, from the most narrow to the widest ones, correspond to the radius of the circle of 1, 2, 3, 4, 5, and 6 fm, respectively. The original spot position is selected to be at the edge of the nuclei. The distribution is calculated for a particle of $p_t = 1$ GeV and fixed freeze-out $T_f = 165$ MeV.

- The blue line is how asimuthal distribution would look like **for sound cylinders, double peak because of two points where the circle crosses the FO surface**

- **The circles were found and studied by Hama,Grassi et al in event-by-event hydro**

The sound cylinders and two horns

(hydro by the Brazilian group, Andrade, Grassi et al)

Origin of the two peaks

Tube “sinks” and matter around “rises” forming a hole+two horns

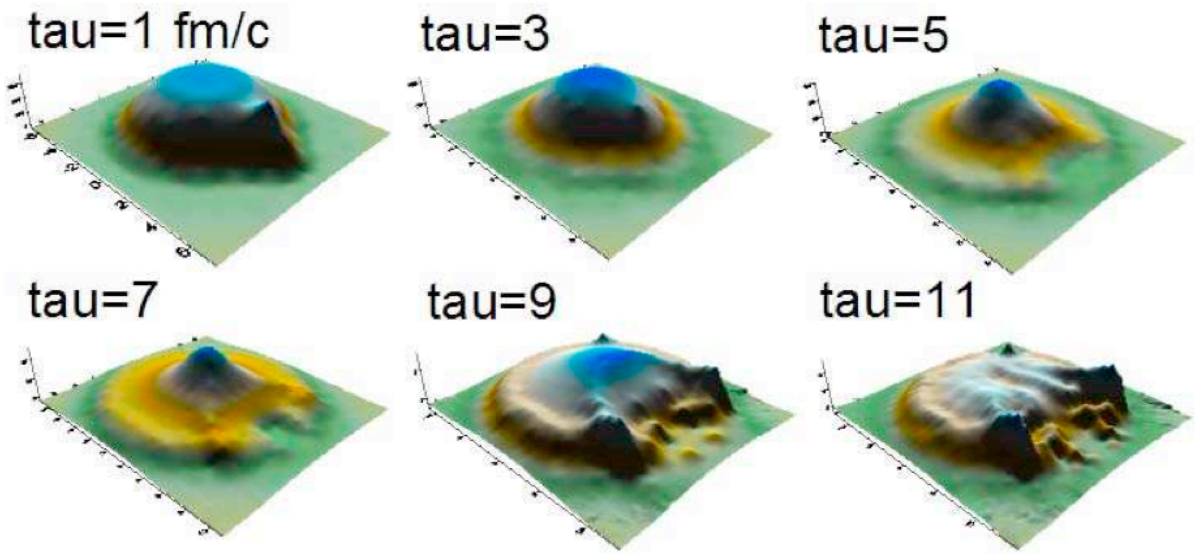

Temporal evolution of energy density for the one tube model.

The peaks are at the same angles +- 1 rad (as I got) from perturbation but **+-2 rad in correlations**

One tube model

MAIN RESULT: single particle angular distribution has TWO PEAKS separated by $\Delta phi \sim 2$

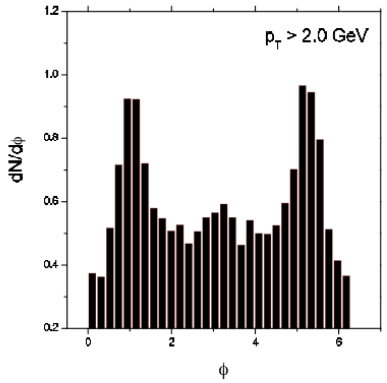

CONSEQUENCE: two particle angular distribution has three peaks

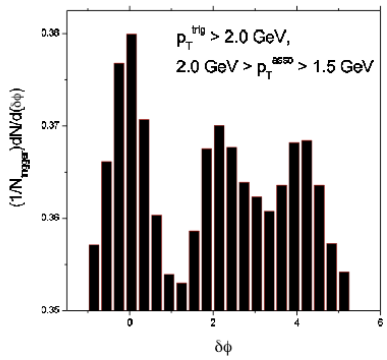

10^9 events
10^6 pairs/event

It is like correlating Two waves in US and Chili to observe tsunami In Japan

S.Gubser, arXiv:1006.0006

found nice solution for nonlinear relativistic axially symmetric explosion of conformal matter

Working in the (τ, η, r, ϕ) coordinates with the metric

$$ds^2 = -d\tau^2 + \tau^2 d\eta^2 + dr^2 + r^2 d\phi^2, \qquad (3.2)$$

and assuming no dependence on the rapidity η and azimuthal angle ϕ, the 4-velocity can be parameterized by only one function

$$u_\mu = (-\cosh\kappa(\tau, r), 0, \sinh\kappa(\tau, r), 0) \qquad (3.3)$$

Omitting the details from [14], the solution for the velocity and the energy density is

$$v_\perp = \tanh\kappa(\tau, r) = \left(\frac{2q^2\tau r}{1 + q^2\tau^2 + q^2 r^2}\right) \qquad (3.4)$$

$$\epsilon = \frac{\hat{\epsilon}_0 (2q)^{8/3}}{\tau^{4/3}\left(1 + 2q^2(\tau^2 + r^2) + q^4(\tau^2 - r^2)^2\right)^{4/3}} \qquad (3.5)$$

$$\tau = \sqrt{t^2 - x^2}$$

$$\eta = (1/2) ln\left(\frac{t + x}{t - x}\right)$$

Kappa is the transverse rapidity

q is a parameter fixing the overall size

The Fate of the Initial State Fluctuations in Heavy Ion Collisions. III The Second Act of Hydrodynamics

Pilar Staig and Edward Shuryak

Comoving coordinates with Gubser flow:

Gubser and Yarom, arXiv:1012.1314

$$\sinh\rho = -\frac{1-q^2\tau^2+q^2r^2}{2q\tau}$$

$$\tan\theta = \frac{2qr}{1+q^2\tau^2-q^2r^2}$$

$$\frac{\partial^2\delta}{\partial\rho^2} - \frac{1}{3\cosh^2\rho}\left(\frac{\partial^2\delta}{\partial\theta^2} + \frac{1}{\tan\theta}\frac{\partial\delta}{\partial\theta} + \frac{1}{\sin^2\theta}\frac{\partial^2\delta}{\partial\phi^2}\right) + \frac{4}{3}\tanh\rho\frac{\partial\delta}{\partial\rho} = 0 \qquad (3.16)$$

We have seen that in the short wavelength approximation we found a wave-like solution to equation 3.16, but now we would like to look for the exact solution, which can be found by using variable separation such that $\delta(\rho,\theta,\phi) = R(\rho)\Theta(\theta)\Phi(\theta)$, then

$$\begin{aligned} R(\rho) &= \frac{C_1 P^{2/3}_{-\frac{1}{2}+\frac{1}{6}\sqrt{12\lambda+1}}(\tanh\rho) + C_2 Q^{2/3}_{-\frac{1}{2}+\frac{1}{6}\sqrt{12\lambda+1}}(\tanh\rho)}{(\cosh\rho)^{2/3}} \\ \Theta(\theta) &= C_3 P_l^m(\cos\theta) + C_4 Q_l^m(\cos\theta) \\ \Phi(\phi) &= C_5 e^{im\phi} + C_6 e^{-im\phi} \end{aligned} \qquad (3.26)$$

where $\lambda = l(l+1)$ and P and Q are associated Legendre polynomials. The part of the solution depending on θ and ϕ can be combined in order to form spherical harmonics $Y_{lm}(\theta,\phi)$, such that $\delta(\rho,\theta,\phi) \propto R_l(\rho)Y_{lm}(\theta,\phi)$.

harmonics l=1..10, Temperature perturbation and velocity

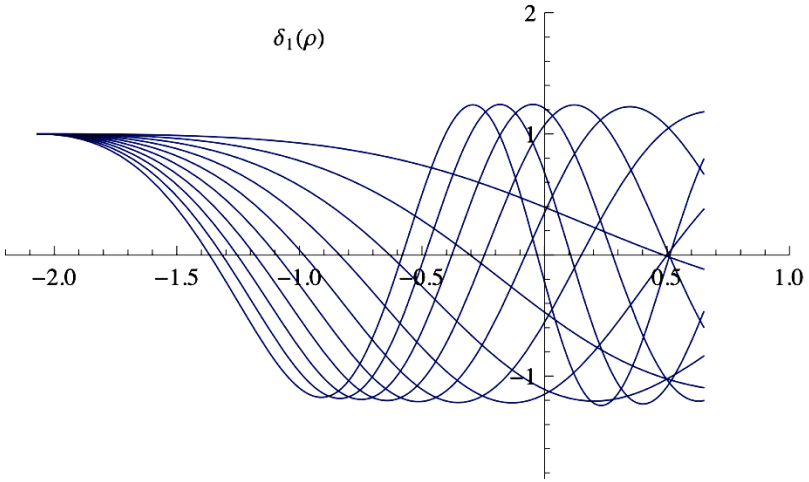

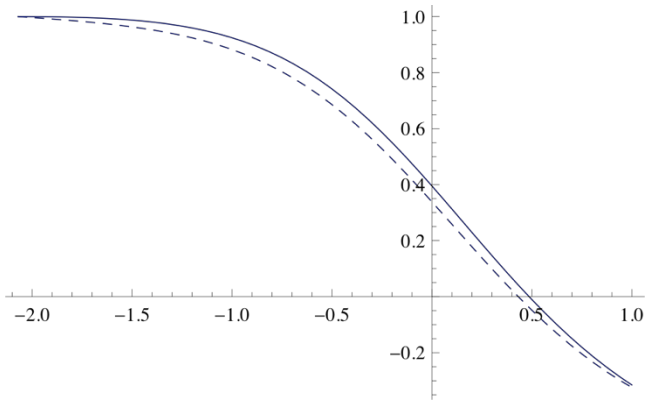

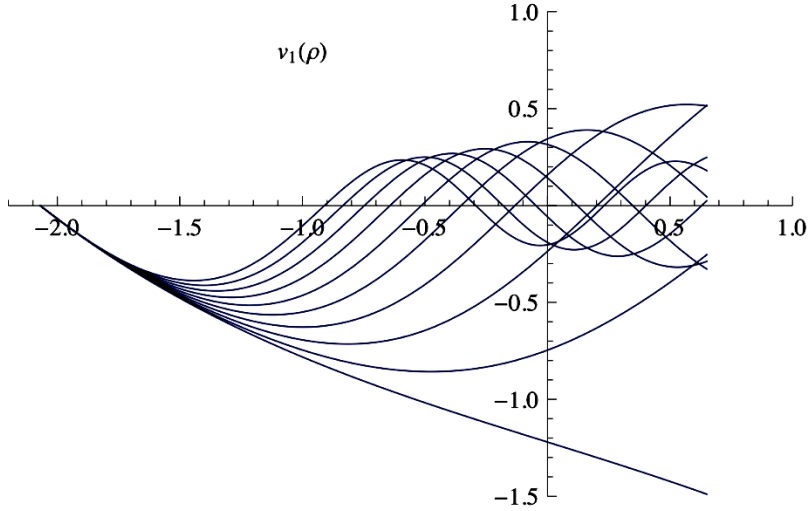

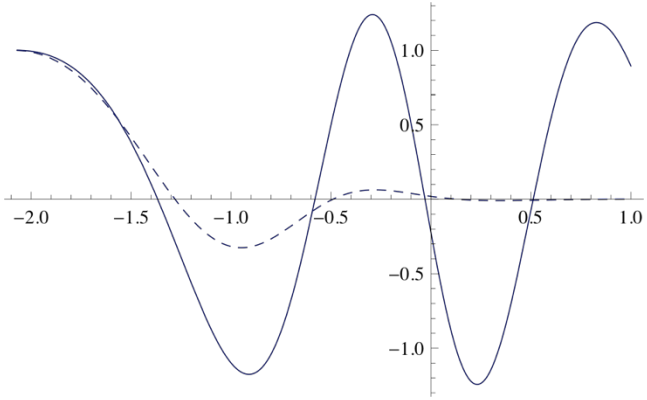

lhs (rho=-2) is initiation time and FO time is around zero

Viscosity (dashed) hardly affect The 1st harmonic, but nearly kills the 10th!

HERE IS THE SUM OF

all (actually 30) HARMONICS

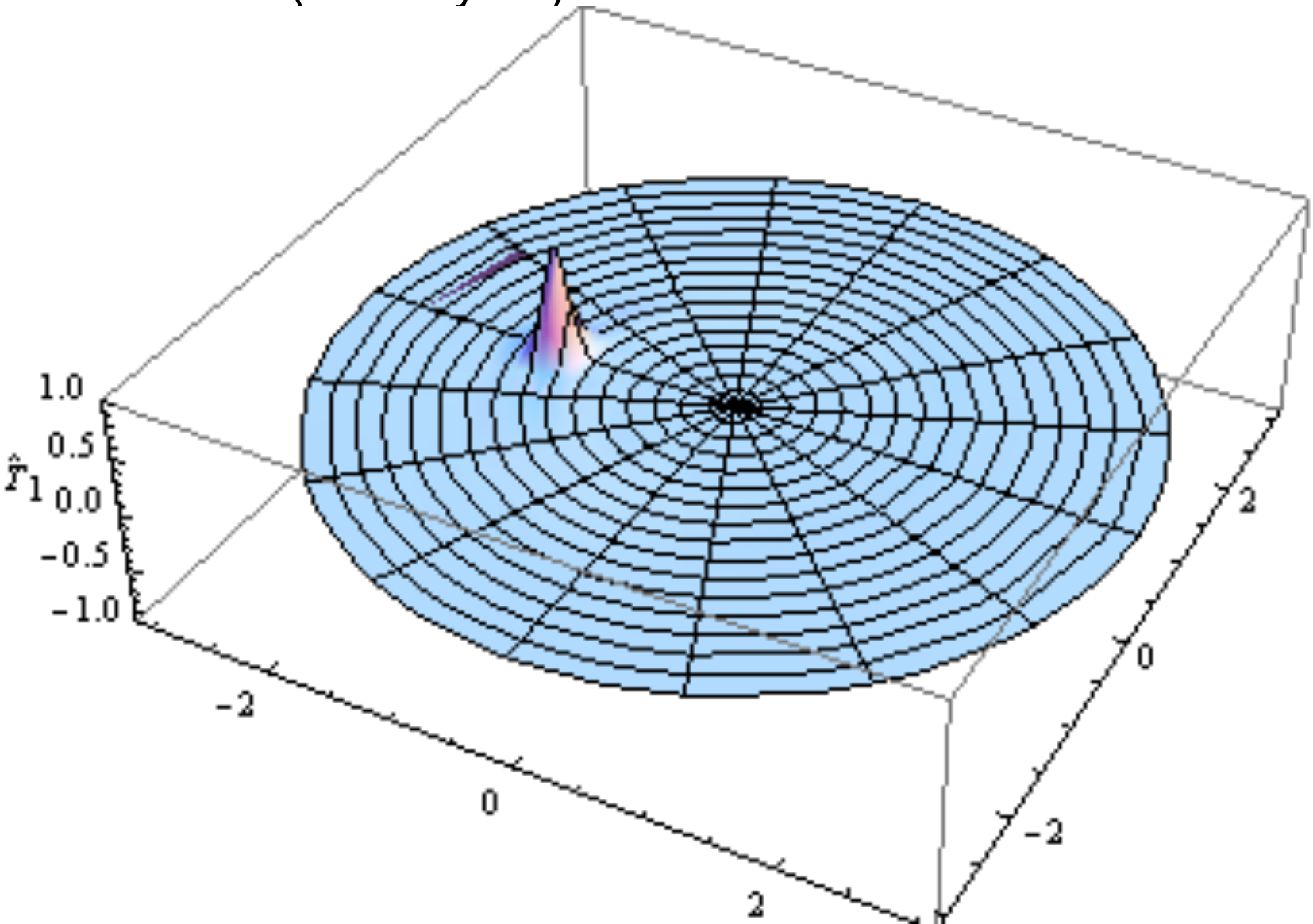

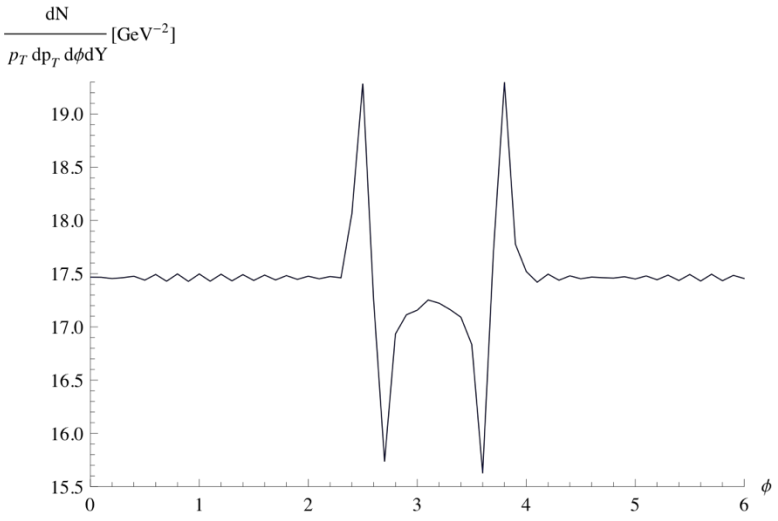

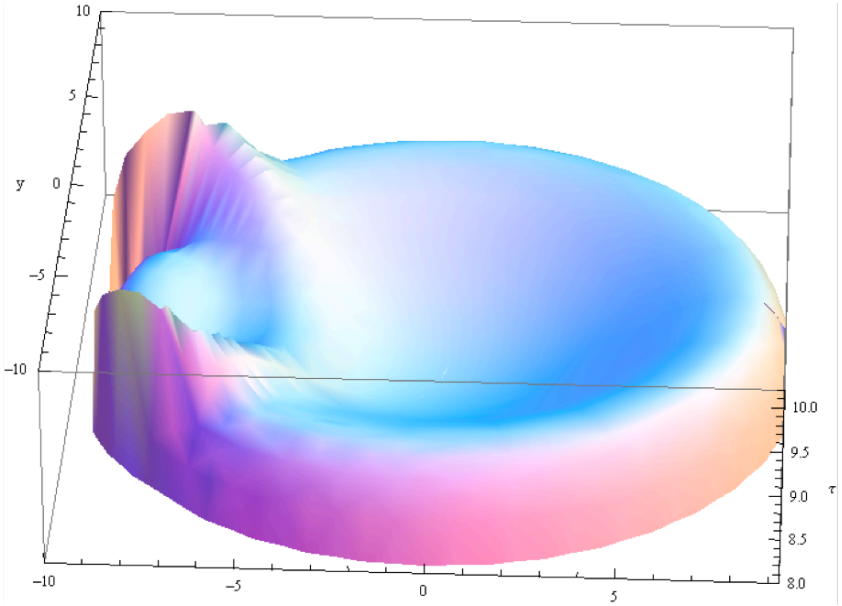

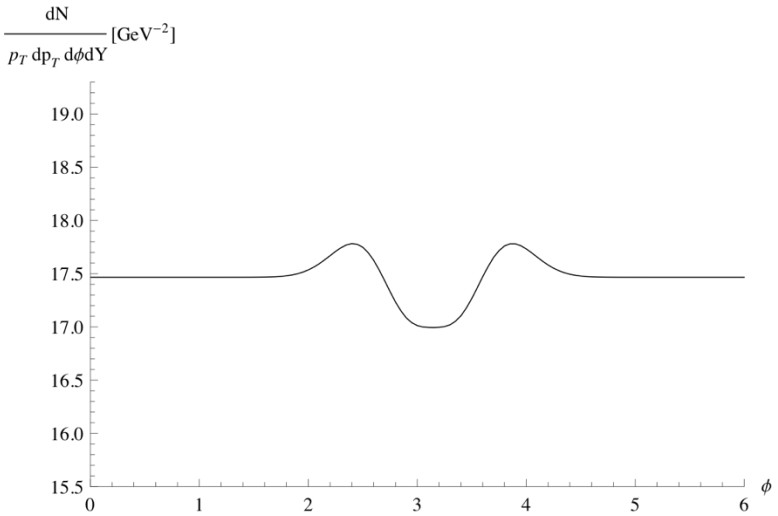

The modified freezeout surface (right) $T=T_f$ (taken to be 120 MeV)

extra area= extra entropy

(in AdS it corresponds to a hologram of a perturbed BH horizon, btw)

A modified angular distribution, with and without viscosity (left)

2 particle correlator vs phi

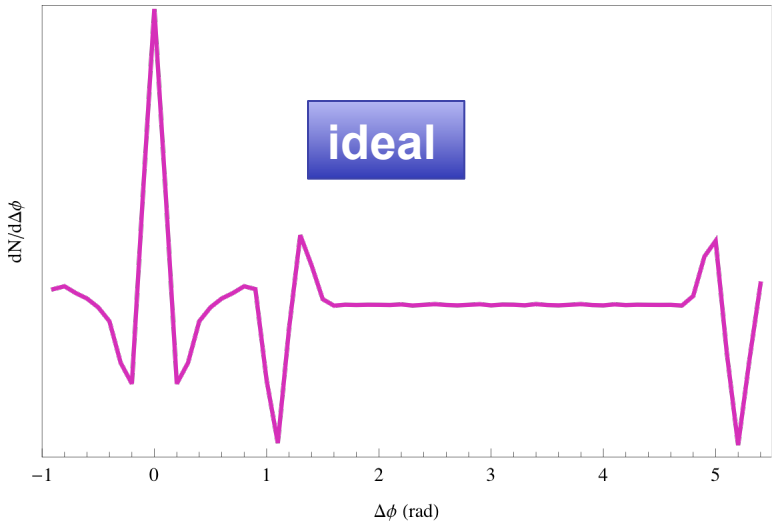

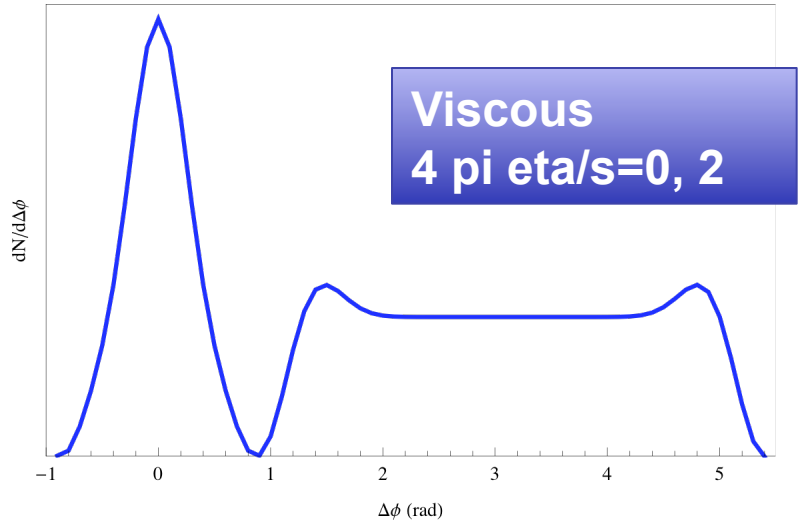

Note shape change

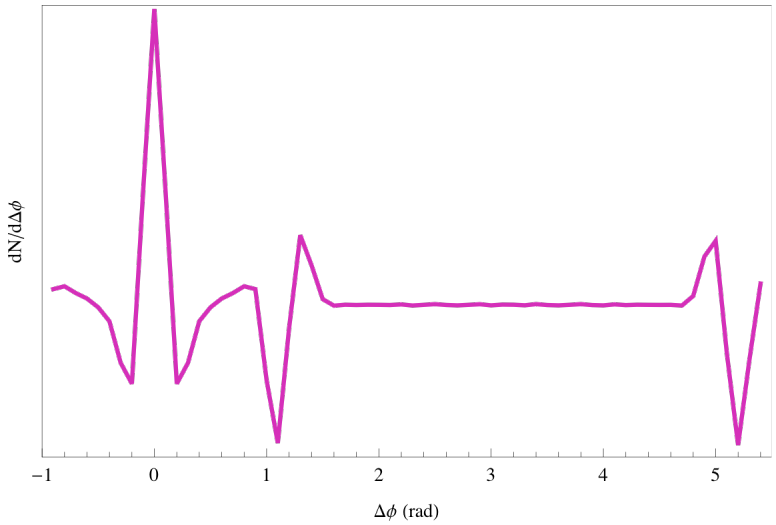

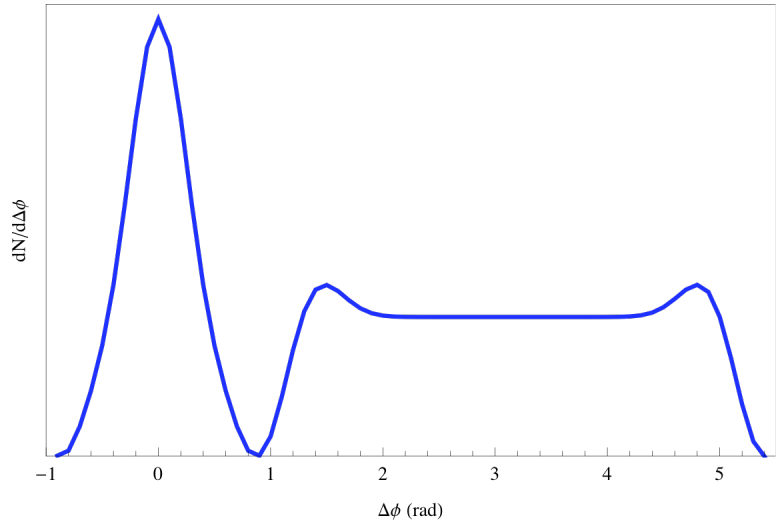

Left:4 pi eta/s=0, 2
Note shape change

ALICE central 1% correlators
Note shape agreement
No parameters, just Green
Function from a delta function

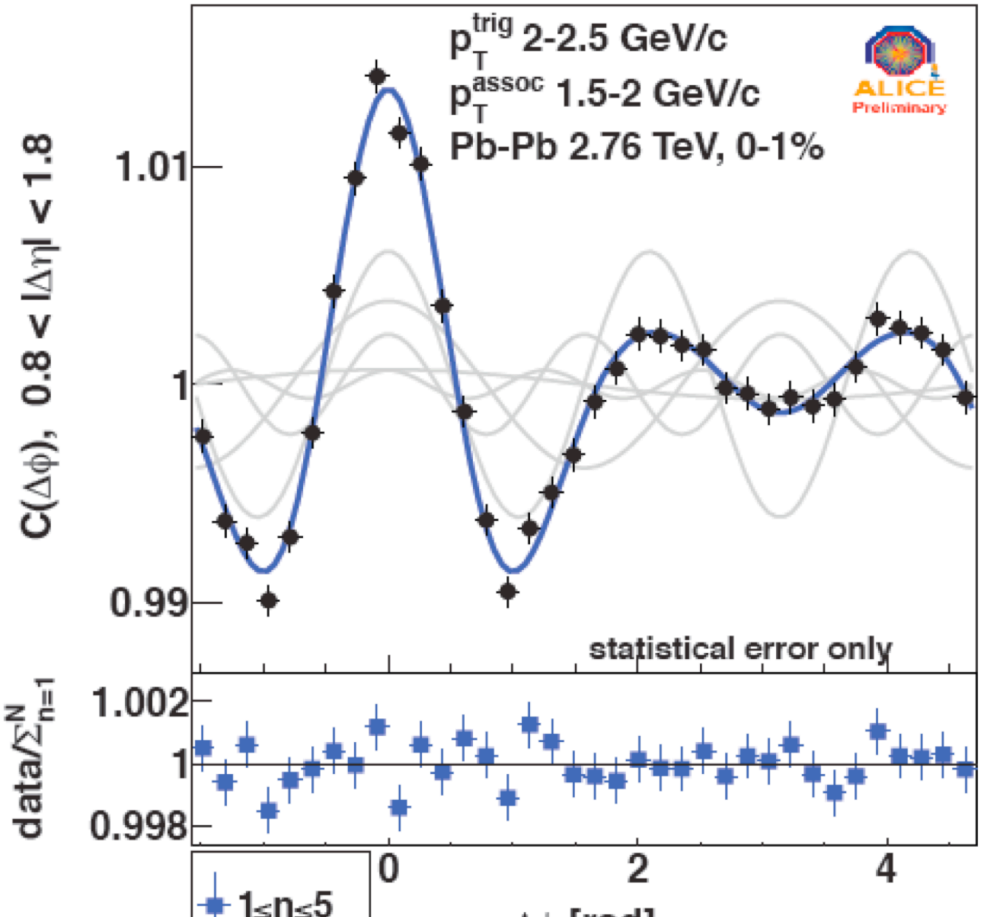

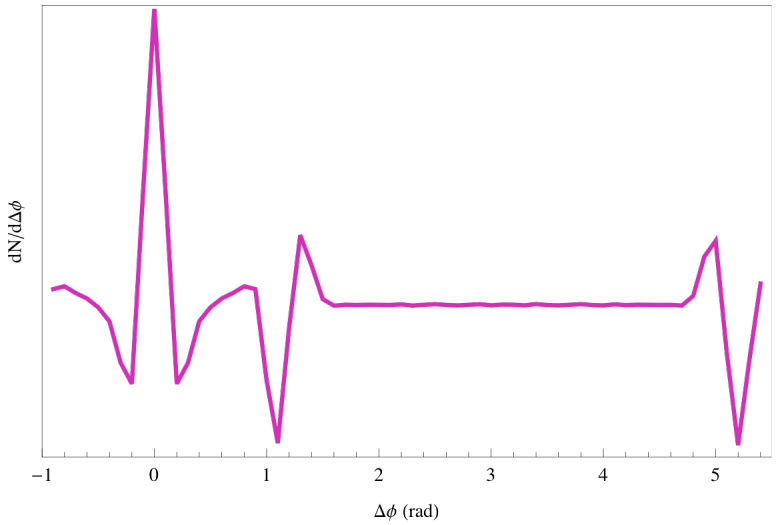

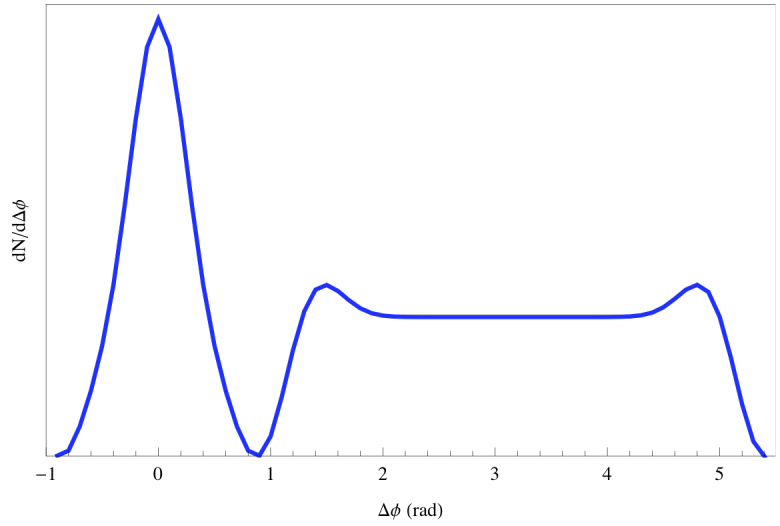

Left:4 pi eta/s=0, 2
Note shape change

ATLAS central 1% correlators
Note shape agreement
No parameters, just Green
Function from a delta function

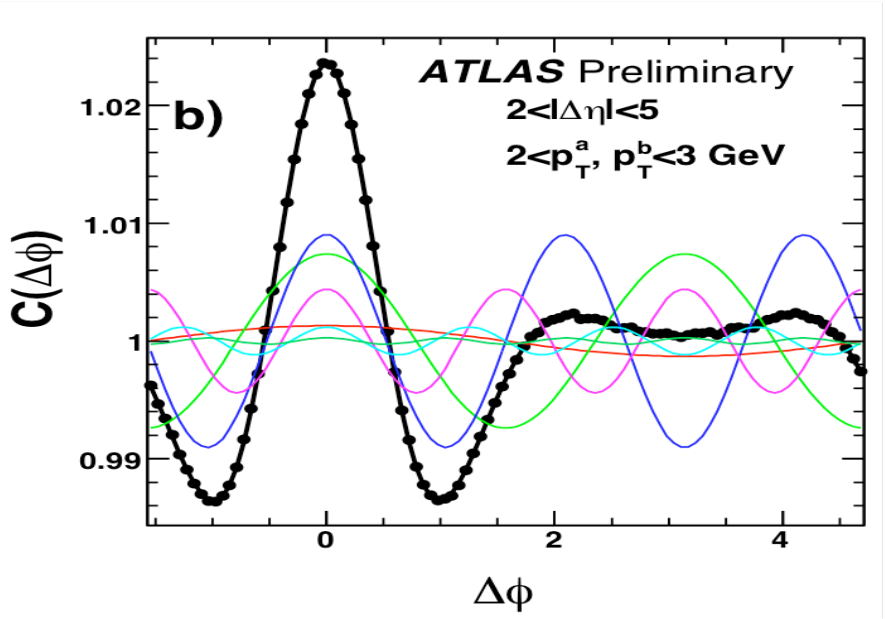

ATLAS data points

The power spectrum has acoustic minima/maxima (at m=7,12 and m=9)

perturbation initial size is 0.7 fm, viscosity eta/s=0,0.08,0.13,0.16

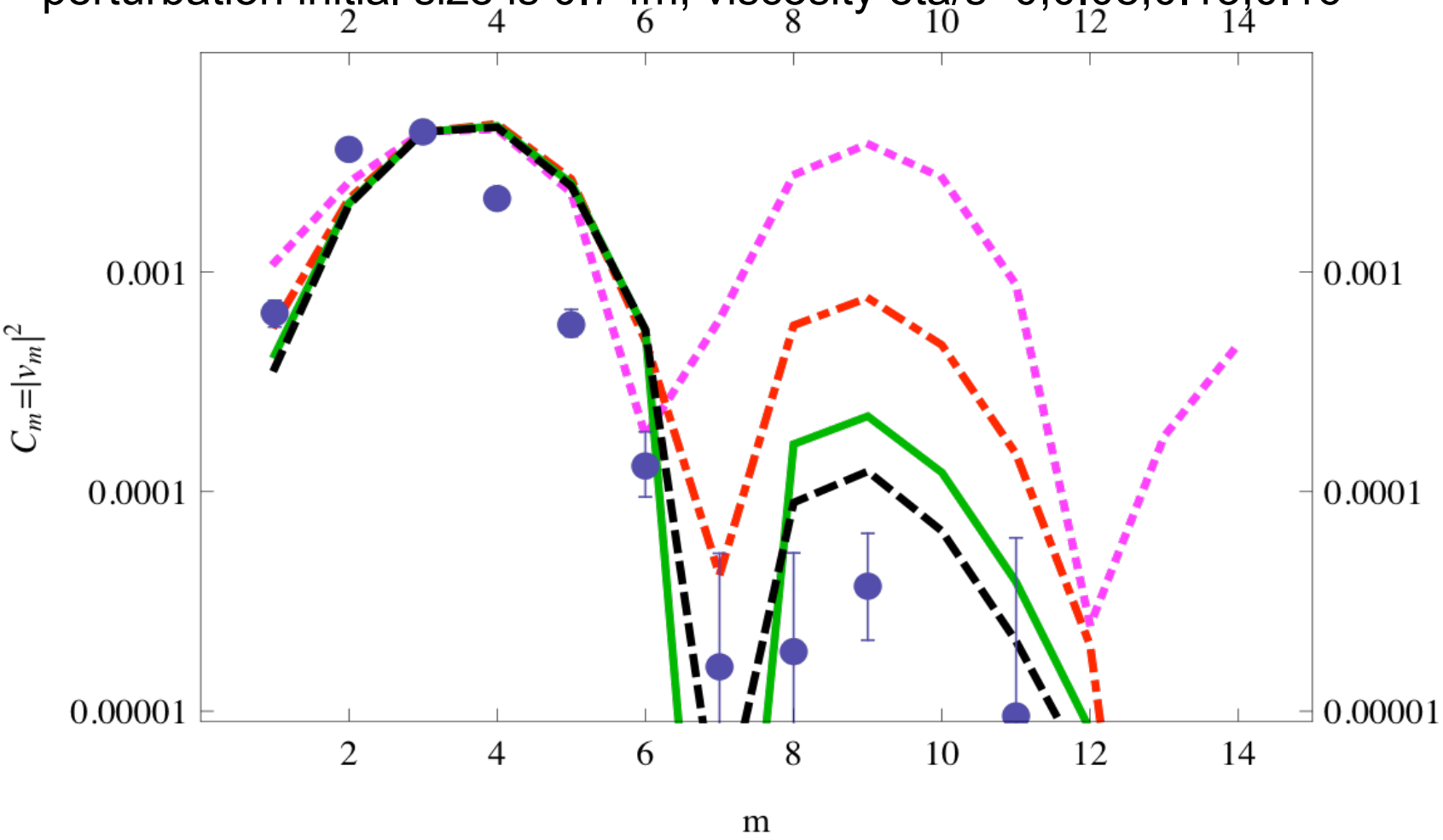

From october CERN Courier, the ALICE power spectrum:

do we see a minimum at n=7?

Maximum at 3 due to 120 degrees peak

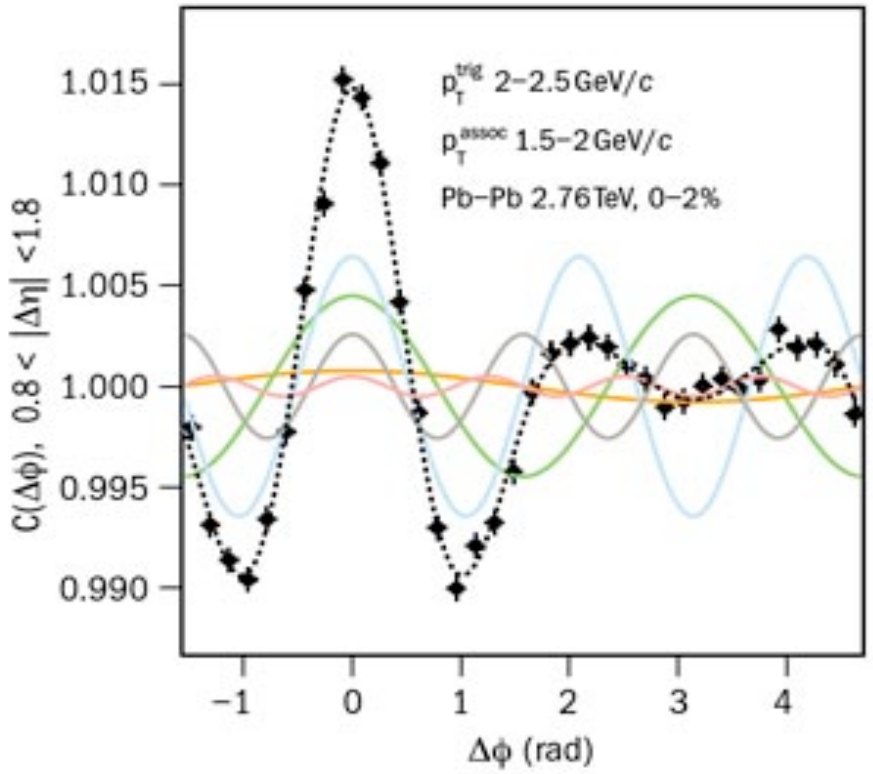

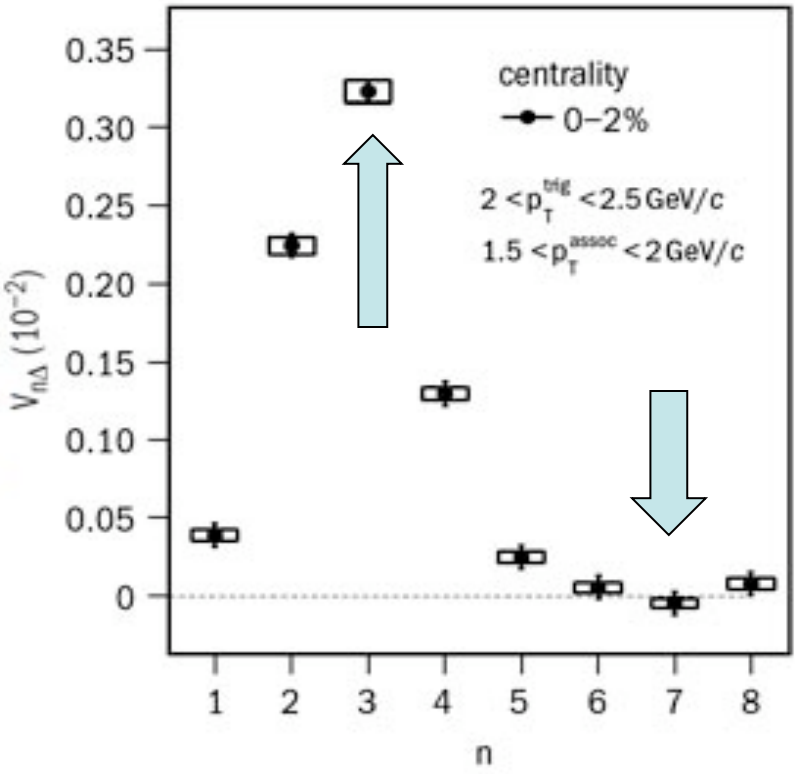

?

So what? Why is hydro's success for the Little Bang interesting/exciting?

•True that already in the 19th century sound vibrations in the bulk (as well as of drops and bubbles) have been well developed (Lord Rayleigh, …)

•But, those objects are macroscopic, they still have 10^20 molecules…

•Little Bang has about 10^3 particles (per unit rapidity) or 10 per dimension. The radial flow well described was already quite surprising: it worked only due to astonishingly small viscosity …

•And now we speak about the 10th harmonics! How a volume cell with O(1) particles can act as a liquid? (well, we look at the surface at freezeout, 2piR about 50 fm, so even 1/10 of it is 5fm…
•Comment: so far the agreement is limited not by a hydro failure, but because of limited experimental statistics!

Are various harmonics coherent?

- **Minimal Gaussian model <=**
- **No coherence, the power plot P(<v_m^2>) is all we can possibly know about them**

Both for the Big and Little bangs the degree of coherence/ non-gaussianity is yet to be determined!

The "maximal coherence" model:

All harmonics come from the same local perturbation and are thus coherently add to ``circles"

Evidences for that From the Glauber model

Before going to AdS/CFT,
a comment on strongly coupled plasmas

- AdS/CFT limit is g^2N is large because N is very large
- Electric-magnetic duality $(\frac{g_E^2}{4\pi})(\frac{g_M^2}{4\pi}) = 1$
- In QCD at T=(1-2)Tc both are about 1
  n(gluons)=n(monopoles)
- Particle-monopole scattering makes small mean free path
- Recent discovery by lattice: at Nf=O(10) one finds **"the most strongly coupled plasma" with $g^2/4\pi$=2-3: is it magnetic-dominated? Is it as good a liquid?**

Thermalization and AdS/CFT

Toward the AdS/CFT Gravity Dual for High Energy Collisions: II. The Stress Tensor on the Boundary

Shu Lin and Edward Shuryak

Department of Physics and Astronomy, Stony Brook University , Stony Brook NY 11794-3800, USA

(Dated: November 25, 2007)

In this second paper of the series we calculate the stress tensor of excited matter, created by "debris" of high energy collisions at the boundary. We found that massive objects ("stones") falling into the AdS center produce gravitational disturbance which however has *zero* stress tensor at the boundary. The falling open strings, connected to receeding charges, do produce a nonzero stress tensor which we found analytically from time-dependent linearized Einstein equations in the bulk. It corresponds to exploding non-equilibrium matter: we discuss its behavior in some detail, including its internal energy density in a comoving frame and the "freezeout surfaces". We then discuss what happens for the ensemble of strings.

If colliding objects are made of heavy quarks moved by an "invisible hand" with +/- v

- Stretching strings are falling under the AdS gravity
- Small v -``modified Ampere" law
- **(Instability** of simple scaling solution and numerical studies)
- In this paper, the

calculation of the **hologram of the falling string**

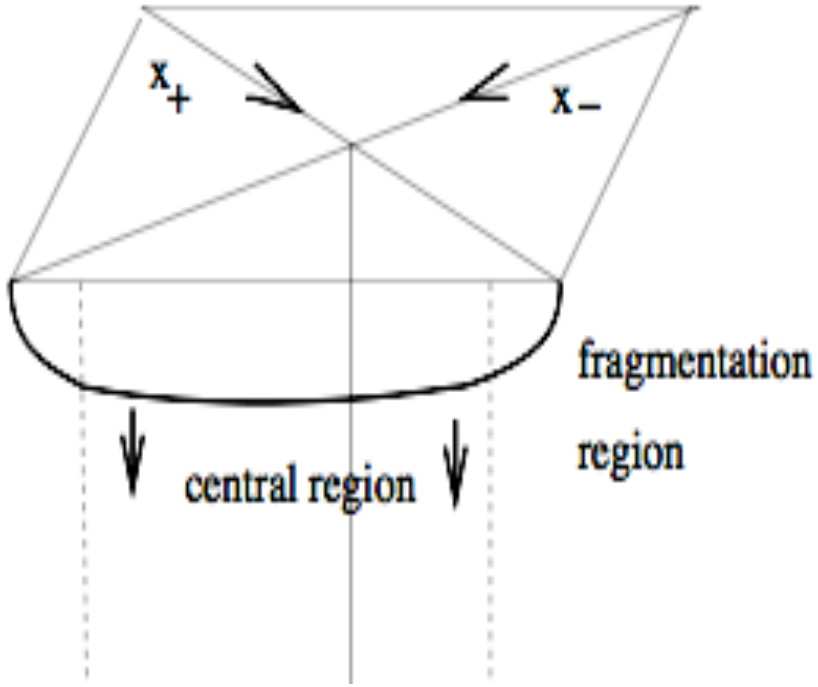

- Holographic imag of a falling string
- *(as far as we know the first time-dependent hologramm)*
- T_{00} , T_{oi}

- **No jets!**
- **Yet it cannot be represented by hydrodynamical explosion => anisotropic pressure in the ``comoving frame”**

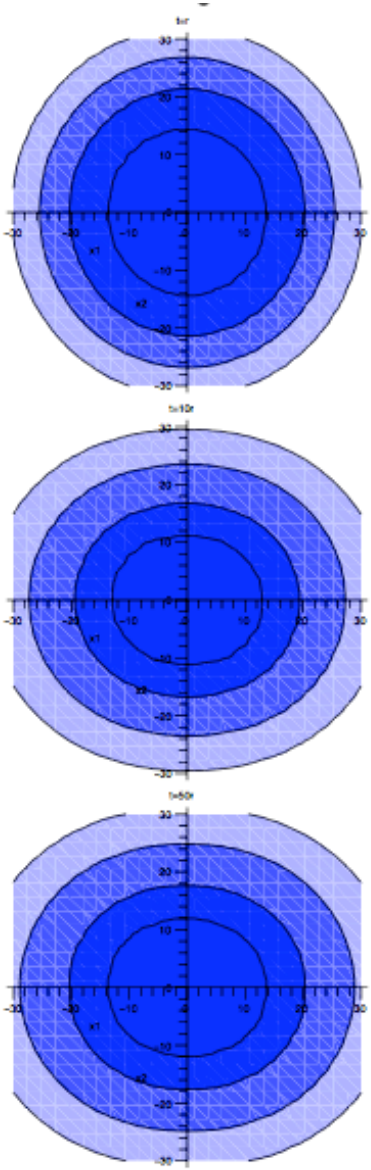

FIG. 1: (color online) The contours of energy density T^{00}, in unit of $\frac{2\sqrt{\lambda}}{f_0^3\pi^2}$, in $x_1 - x_2$ plane at different time. The three plots are made for $t = r$, $t = 10r$ and $t = 50r$ from top to bottom. The magnitude of T^{00} is represented by the color,

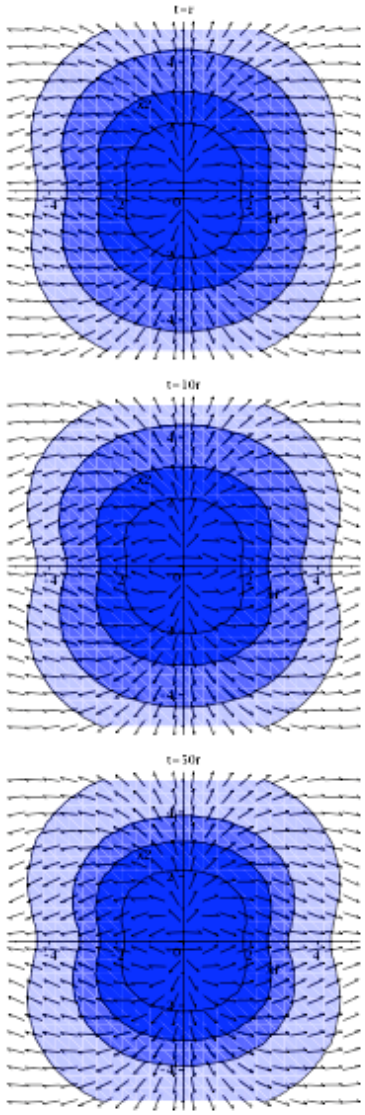

FIG. 2: (color online)The contours of momentum den sity T^{0i}, in unit of $\frac{2\sqrt{\lambda}}{f_0^3\pi^2}$, in $x_1 - x_2$ plane at differen time. The three plots are made for $t = r$, $t = 10$ and $t = 50r$ from top to bottom. The magnitude i represented by color, with darker color corresponding t greater magnitude. The corresponding contour values ar

The story of two membranes:

(Many strings falling together)

- Imagine 2 walls of heavy quarks => multiple strings falling (e.g.no dependence on transverse coordinates x_2,x_3)
- The object is thus not a string but **3d membrane creating horizon from its own weight**
- => not to be confused with membrane of the "membrane paradigm" hovering just above the horizon

Toward the AdS/CFT Gravity Dual for High Energy Collisions. 3.Gravitationally Collapsing Shell and Quasiequilibrium

Phys.Rev.D78: 125018,2008. arXiv:0808.0910

Shu Lin[1], and Edward Shuryak[2]

The main simplification of the paper is that this shell is *flat* - independent on our world 3 spatial coordinates. Therefore the overall solution of Einstein eqns reduces to two separate regions with well known *static* AdS-BH and AdS metrics. The falling of the shell is time dependent, its equation of motion is determined by the Israel junction condition, which we solve and analyzed. We also determined how final temperature (horizon position) depends on initial scale and shell tension.

- Falling is dual to

further equilibration UV=>IR

This is *quasiequilibrium* in the title. More specifically it means the following. In this geometry a "single point observer" – who is only able to measure the *average density and pressure* – would be driven to the conclusion that the matter is instantaneously equilibrated at *all* times. However more sophisticated "two point observer" who is able to study correlation functions of stress tensors would be able to observe deviations from the thermal case. We computed them explicitly, calculating a number of spectral densities at various positions of the shell, corresponding (in quasi-static approximation) to different stages of equilibration.

Two types of observers

- Single-point observer sees thermal stress tensor with T=const(t)
- Nonlocal 2-point experiments (the stress tensor correlators) send signal into the bulk and finds deviations: equilibration is actually time dependent

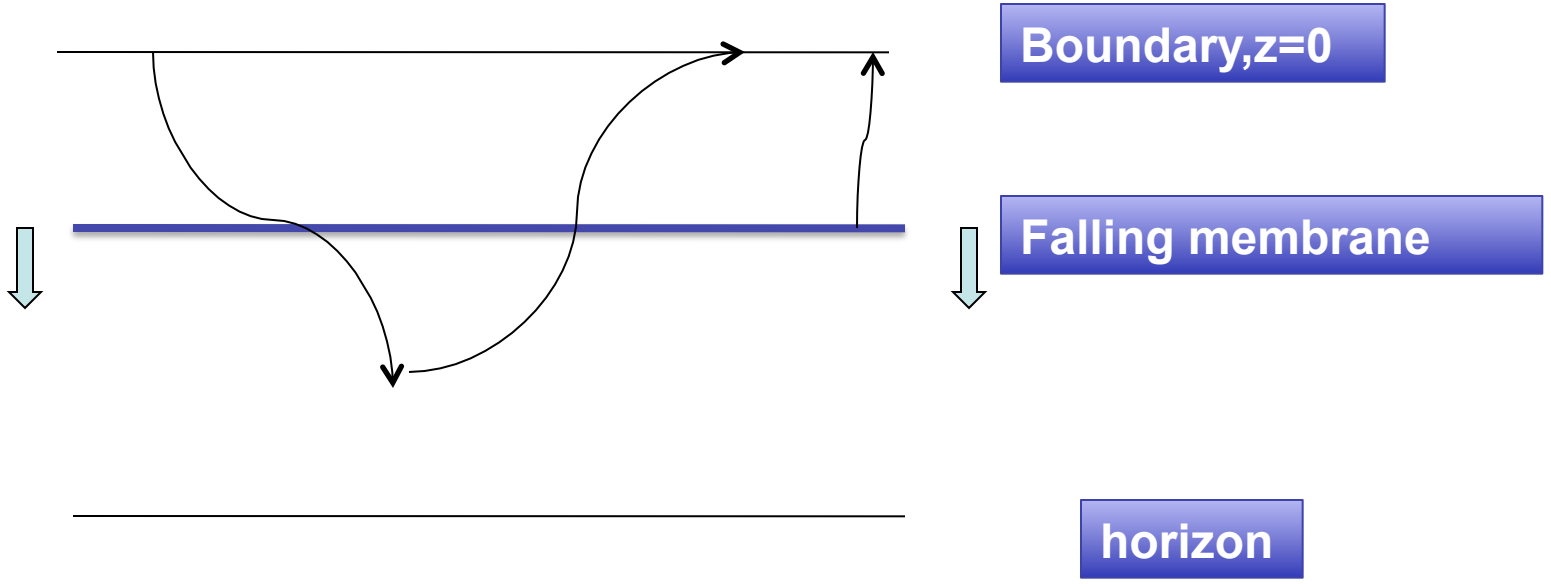

Israel's junction condition is dual to the equilibration dynamics

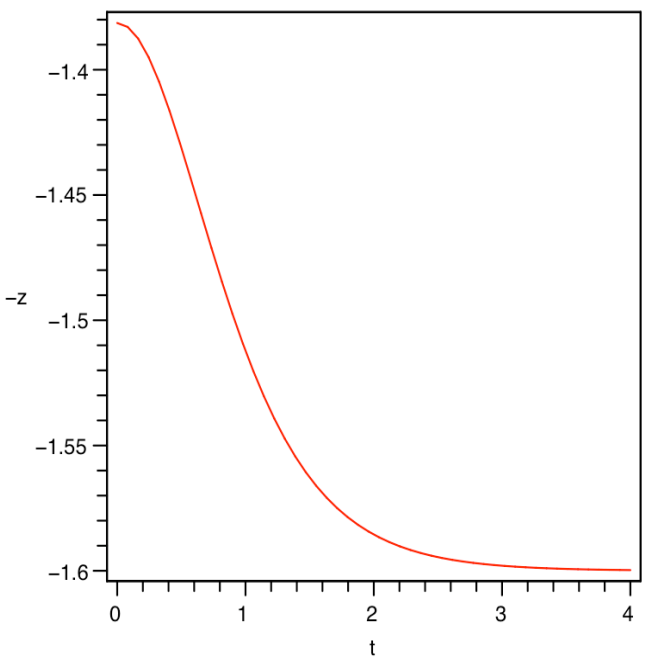

- Thermal AdS above= UV is equilibrated
- Cold AdS5 below= IR is not equilibrated
- The equilibration front moves

$$\frac{dz}{dt} = \frac{\dot{z}}{\dot{t}} = \frac{f\sqrt{(\frac{\kappa_5^2 p}{6})^2 + (\frac{3}{2\kappa_5^2 p})^2(1-f)^2 - \frac{1+f}{2}}}{\frac{\kappa_5^2 p}{6} + \frac{3}{2\kappa_5^2 p}(1-f)}$$

$$f = 1 - (z/z_h)^4$$

Average T_{ij} is thermal but the correlators (the two-point observers) deviate from equilibrium: (depending on q)

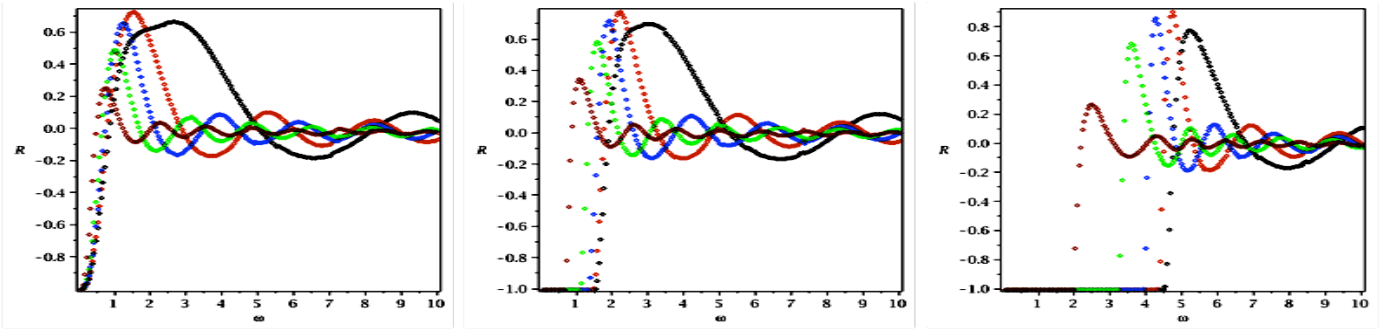

Figure 3: (color online)The relative deviation R at $q = 0$ left, $q = 1.5$ middle and $q = 4.5$ right. Different stages of thermalization are indicated by: black($u_m = 0.1$), red($u_m = 0.3$), blue($u_m = 0.5$), green($u_m = 0.7$), brown($u_m = 0.9$). As u_m approaches 1, i.e. the medium evolves to equilibrium, the oscillation decreases in amplitude and increases in frequency, thus the spectral density relaxes to thermal one

The reason for oscillations in spectral densities is in fact the ``echo" effect, induced by a gravitons scattering from a membrane, Confirmed numerically and semiclassically

Entropy production

estimates of area of trapped surface

A signifcant leap forward had been done recently by Gubser, Pufu and Yarom [123], who proposed to look at heavy ion collision as a process of head-on collision of two point-like black holes, separated from the boundary by some depth L – tuned to the nuclear size of Au to be about 4 fm, see Fig.??. By using global AdS coordinates, these authors argued that (apart of obvious axial O(2) symmetry) this case has higher – namely O(3)– symmetry with the resulting black hole at the collision moment at its center, thus in certain coordinate

$$q = \frac{\vec{x}_\perp^2 + (z-L)^2}{4zL} \tag{91}$$

the 3-d trapped surface C at the collision moment should be just a 3-sphere, at constant $q = q_c$. (Here $x_\perp$ are two coordinates transverse to the collision axes.) The picture of it is shown in Fig.29(b)

If so, one can find the radius at which it is the trapped null-surface and determine its energy and Bekenstein entropy. For large q_c these expressions are

$$E \approx \frac{4L^2 q_c^3}{G_5}, \quad S \approx \frac{4\pi L^3 q_c^2}{G_5}, \tag{92}$$

from which, eliminating q_c, the main result of the paper follows, namely that the entropy grows with the collision energy as

$$S \sim E^{2/3} \tag{93}$$

Note that this power very much depends on the 5-dimentional gravity and is different from the 1950's prediction of Fermi and Landau (??) in which this power was 1/2 and (accidentally or not) fits the data better.

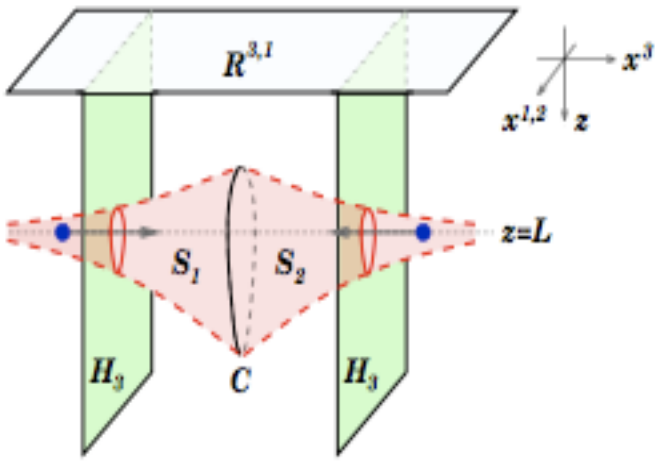

- Gubser,Pufu and Yarom" Heavy ion collisions as that of two black holes

What is L? (bh positions in the holographic direction)

- Gubser et al: L is dual to the nuclear size, so it is O(10 fm)
- Lin,ES: L=1/Qs, the partonic scale in nuclei, so it is O(0.1 fm) thermalization

Should be **falling down** to horizon 1/(pi T)

$$L \sim 1/Q_s \sim 1/E^{1/4}$$

$$S \sim E^{2/3} L^{5/3} \sim E^{1/4}$$

Experiment:
pp $E^{0.22}$
AA $E^{0.30}$

Grazing Collisions of Gravitational Shock Waves and Entropy Production in Heavy Ion Collision

Shu Lin[1], and Edward Shuryak[2]

The shock wave moving in $+x^3$ direction is given by:

$$ds^2 = L^2 \frac{-dudv + (dx^1)^2 + (dx^2)^2 + dz^2}{z^2} + L\frac{\Phi(x^1, x^2, z)}{z}\delta(u)du^2$$

with $\Phi(x^1, x^2, z)$ satisfies the following equation:

$$\left(\Box - \frac{3}{L^2}\right)\Phi = 16\pi G_5 J_{uu}$$

The vanishing of expansion gives the equation:

$$\left(\Box - \frac{3}{L^2}\right)(\Psi_1 - \Phi_1) = 0$$

$$\Psi_1|_{\mathcal{C}} = \Psi_2|_{\mathcal{C}} = 0$$

The boundary $\mathcal{C}$ should be chosen to satisfy the constraint:

$$\nabla\Psi_1 \cdot \nabla\Psi_2|_{\mathcal{C}} = 4$$

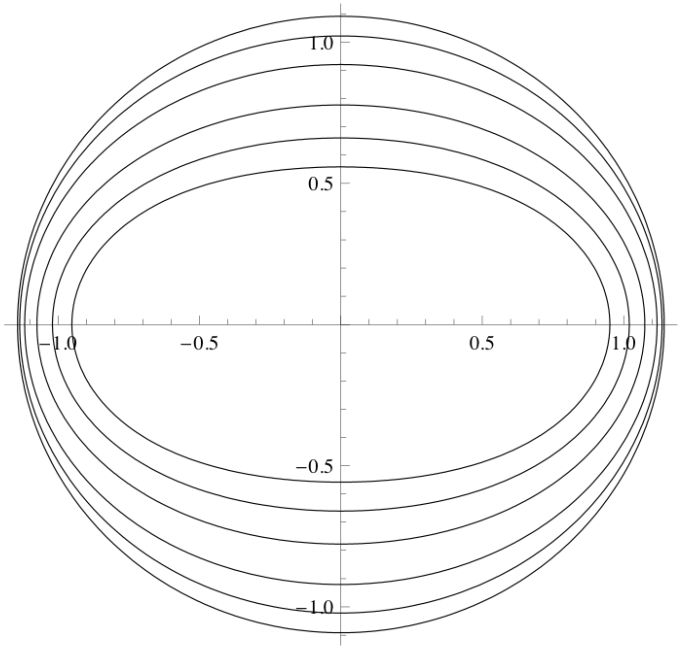

Off-center collisions in AdS_5 with applications to multiplicity estimates in heavy-ion collisions

Steven S. Gubser,* Silviu S. Pufu,† and Amos Yarom‡

Joseph Henry Laboratories, Princeton University, Princeton, NJ 08544, USA

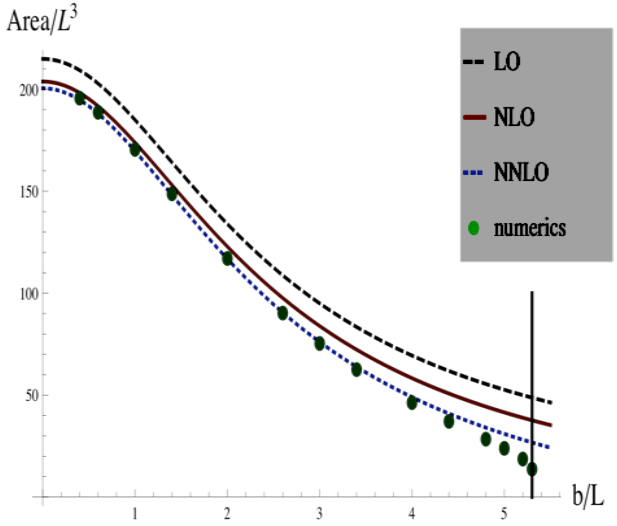

Figure 1: (Color online.) Comparisons between the numerics of [36] and the analytic formula (58). The black dashed curve represents the leading term in (58); the solid red curve corresponds to the first two terms in (58); the dotted blue curve represents the expression (58), which is correct up to a term of order $\mathcal{O}(1/\zeta^2)$; the green dots represent the numerical evaluations used in figure 3 of [36]; lastly, the vertical green line marks the place where, according to [36], the maximum impact parameter $b_{\max}/L$ occurs. We thank S. Lin and E. Shuryak for providing us with the results of their numerical evaluations.

The entropy vs the impact parameter:

Points from Lin+ES

Note nonzero value at the end

black hole disappears with a jump! What is striking: **we see something similar in experiment**

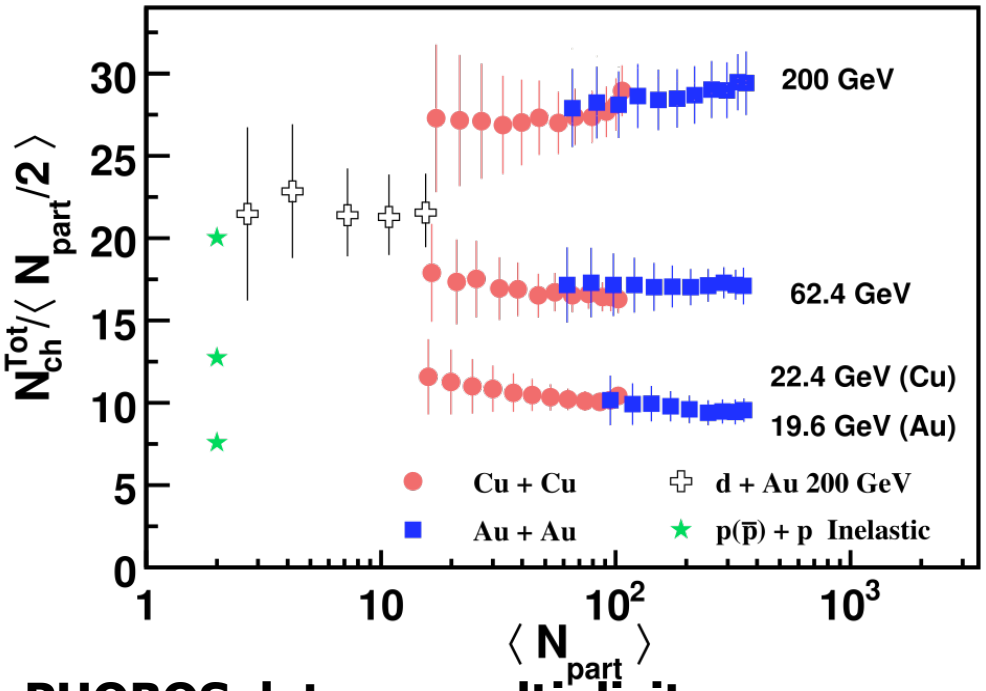

PHOBOS data on multiplicity hint for a jump but do not really show it

Not-too-peripheral AA, with hydro, Has one multiplicity

pp,pA and very peripheral AA has another

On the critical condition in gravitational shock wave collision and heavy ion collisions

Shu Lin[a1], and Edward Shuryak[b2]

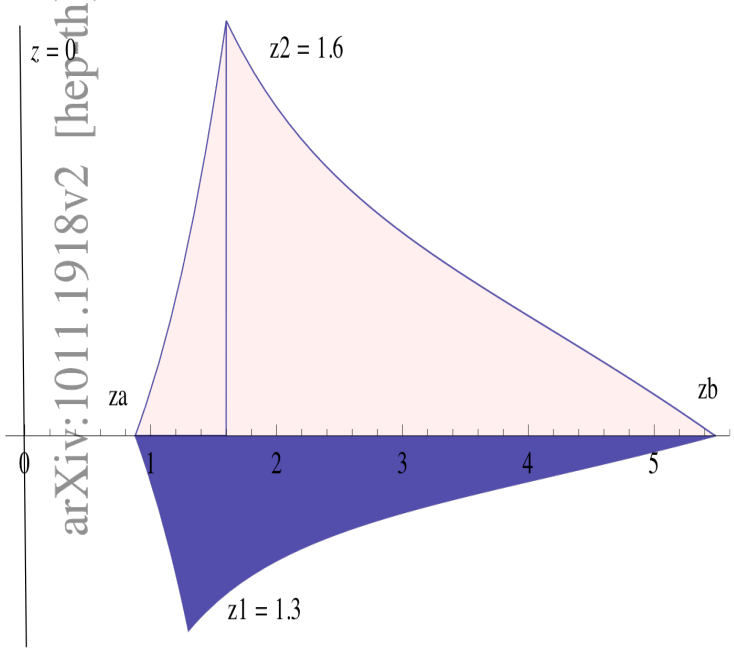

$$z^2\Psi_i'' - z\Psi_i' - 3\Psi_i = -16\pi G_5 \mu_i z_i^4 \delta(z - z_i)$$

$$\Psi_i(z_a) = \Psi_i(z_b) = 0$$

$$\Psi_1'(z_a)\Psi_2'(z_a)\frac{z_a^2}{L^2} = \Psi_1'(z_b)\Psi_2'(z_b)\frac{z_b^2}{L^2} = 4$$

Wall-on-wall collision
Walls are sourced by point bulk objects resigning at z_1,z_2

The trapped surface reduces To two points z_a, z_b are Obtained from a complcated algebraic eqns, which has solution for any z_1,z_2

Figure 3: (color online)A view of the outer-most trapped surface formation in a wall-on-wall collision with two sources at different depths. The pink and blue area indicate the growth of the trapped surface Ψ in the bulk. The sources of the shock waves lie at $\frac{z_1}{L} = 1.3$ and $\frac{z_2}{L} = 1.6$, and the energy density is fixed by $\frac{(8\pi G_5 \mu)^2 (z_1 z_2)^3}{L^3} = 20$. The trapped surface at the collision point is bounded by z_a and z_b

LHC jets and their quenching

Much more energetic jets and stronger quenching is found at LHC!

ATLAS, 1st PRL on heavy ions, Accepted in one (Thanksgiving!) day

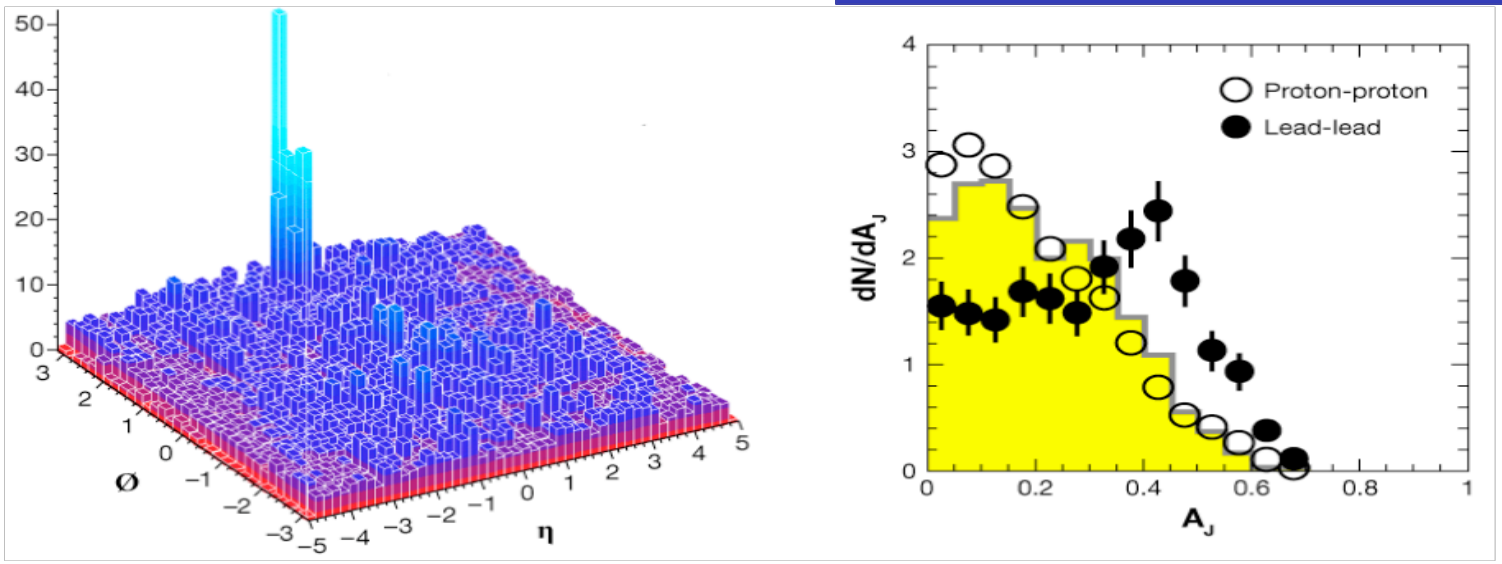

FIG. 2: (Left) Example of a jet without a visible partner. (Right) Asymmetric jets (where one jet loses most of its energy) are rare in proton-proton collisions, but the ATLAS measurements showed such events occur with a high probability in lead-lead collisions. The asymmetry A_j for two jets with energy E_1 and E_2 is defined as $A_j = (E_1 - E_2)/(E_1 + E_2)$. (Credit: G. Aad *et al.*, [2])

Basic questions on jet quenching (not yet answered…)

- Is it due to the color charge or **energy**?
- Is it pQCD, radiation of gluons, or **AdS/CFT, radiation of gravitons (sounds)**?
- Are there the **transverse kicks** vs **longitudinal classical braking force?**

Even very asymmetric events have back-to-back geometry
The braking force seem to be the case…

The vertical axis is Extra 5th dimension Means scale in the renormgroup sense

Light quark energy loss in strongly-coupled $\mathcal{N}=4$ supersymmetric Yang-Mills plasma

Paul M. Chesler*, Kristan Jensen†, Andreas Karch‡, and Laurence G. Yaffe§
Department of Physics, University of Washington, Seattle, WA 98195, USA
(Dated: July 21, 2009)

We compute the penetration depth of a light quark moving through a large N_c, strongly coupled $\mathcal{N}=4$ supersymmetric Yang-Mills plasma using gauge/gravity duality and a combination of analytic and numerical techniques. We find that the maximum distance a quark with energy E can travel through a plasma is given by $\Delta x_{\rm max}(E) = (\mathcal{C}/T)\,(E/T\sqrt{\lambda})^{1/3}$ with $\mathcal{C} \approx 0.5$.

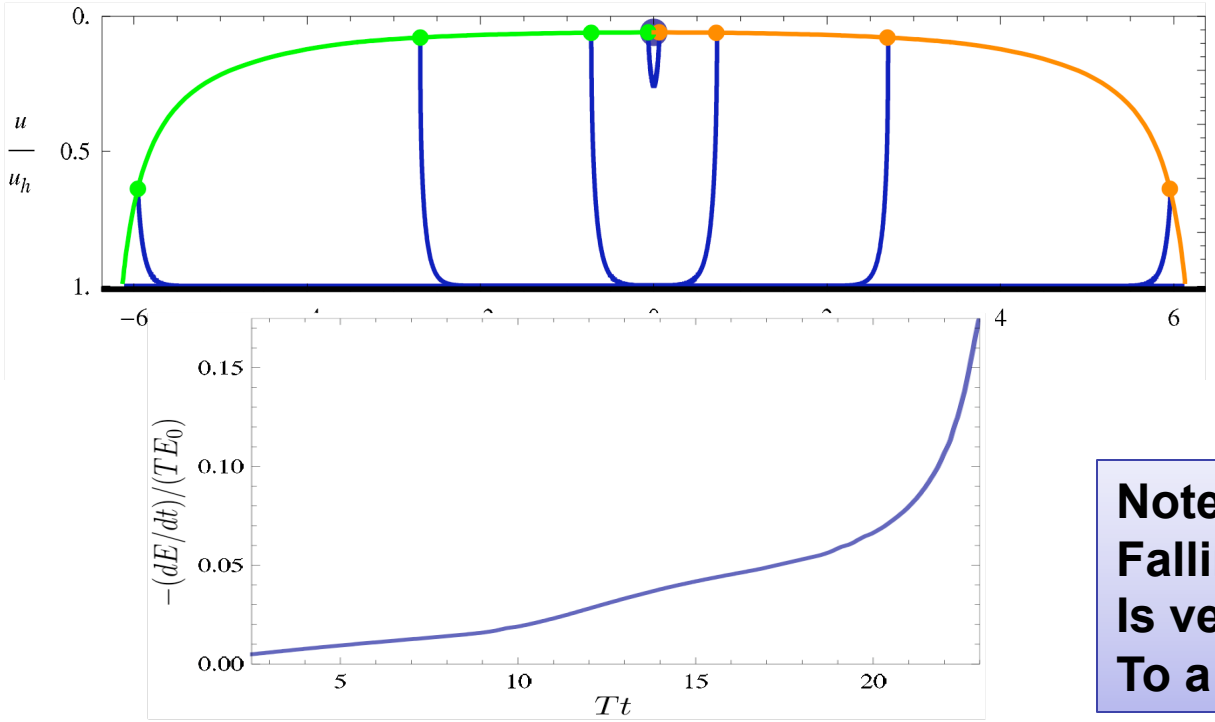

FIG. 7: The instantaneous energy loss rate, dE/dt, of a highly energetic quark, normalized by its initial energy E_0. Instead of decreasing with time, as might have been expected, the light quark energy loss rate actually increases. At times near the thermalization time, which for this particular example is $t_{\rm therm} \sim 24/T$, the instantaneous energy loss rate grows like $dE/dt \sim 1/\sqrt{t_{\rm therm} - t}$.

Note: the Falling path Is very close To a geodesic

Geodesics in matter and "hot wind" frames

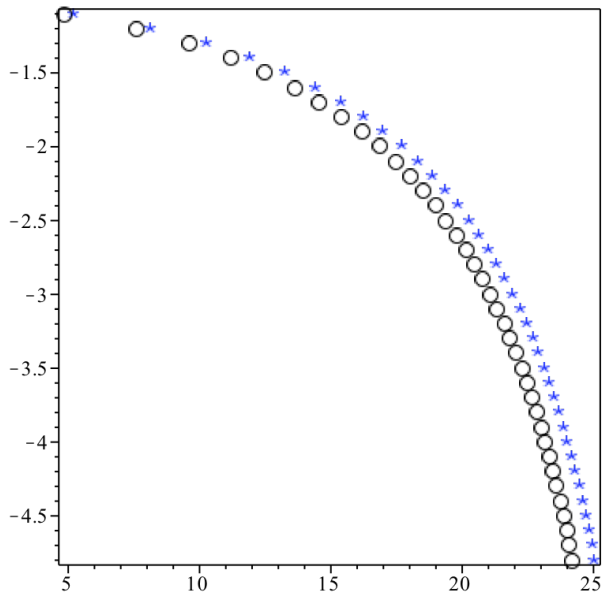

FIG. 1: (color online) Example of a geodesic trajectory for a falling particle in the (inverted) 5-th coordinate $-z$ as a function of x^1. The open (black) circles are for massive particle, blue) asteriks are for massless geodesic. The parameters are explained in the text

The 5d metric has the form

$$ds^2 = \frac{L^2}{z^2}\left(\frac{dz^2}{f} - f dt^2 + d\vec{x}^2\right), \qquad (3.13)$$

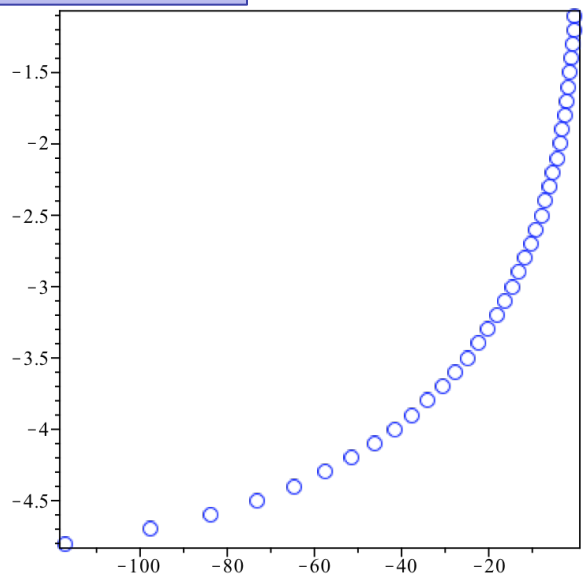

FIG. 3: (color online) The same example of a geodesic trajectory for a falling particle as in the previous figure, but in the boosted "hot wind" frame. The points are in the (inverted) 5-th coordinate $-z$ as a function of x^1, which is now also negative as the "hot wind" blows in the negative direction.

As a result, even if $P = 0$, one gets a nonzero velocity in the x direction since

$$u^0 = g^{00}E, \;\; u^1 = g^{10}E. \qquad (4.9)$$

The upper component metric is obtained in the standard way with

$$u^t = \frac{dt}{d\tau} = E\frac{z^2(z_h^4 + z^4\gamma^2 - z^4)}{z^4 - z_h^4}, \qquad (4.10)$$
$$u^x = \frac{dx}{d\tau} = E\sqrt{\gamma^2 - 1}\frac{z^6}{z^4 - z_h^4}.$$

Jet Quenching via Gravitational Radiation in Thermal AdS

Edward Shuryak, Ho-Ung Yee, and Ismail Zahed

Department of Physics and Astronomy, State University of New York, Stony Brook, NY 11794
(Dated: October 4, 2011)

We argue that classical bulk gravitational radiation effects in AdS/CFT, previously ignored because of their subleading nature in the $1/N_c$-expansion, are magnified by powers of large Lorentz factors γ for ultrarelativistic jets, thereby dominating other forms of jet energy loss in holography at finite temperature. We make use of the induced gravitational self-force in thermal AdS_5 to estimate its effects. In a thermal medium, relativistic jets may loose most of their energy through longitudinal drag caused by the energy accumulated in their nearby field as they zip through the strongly coupled plasma.

D. Cyclotron versus gravitational radiation

The first step toward relating two very different motivations mentioned in the earlier part of introduction has been done by one of us (with Khriplovich) nearly 40 years ago [17], applying the same method to 4 problems: cyclotron electromagnetic/gravitational radiations in flat or curved 3+1 dimensional spaces in the ultrarelativistic regime $\gamma \gg 1$. The results for the radiation intensity are

$$\mathbf{I}^{\rm flat}_{\rm e.m.} \approx e^2\gamma^4/R^2, \qquad \mathbf{I}^{\rm flat}_{\rm grav} \approx G_4 m^2\gamma^4/R^2,$$
$$\mathbf{I}^{\rm curv}_{\rm e.m.} \approx e^2\gamma^2/R^2, \qquad \mathbf{I}^{\rm curv}_{\rm grav} \approx G_4 m^2\gamma^2/R^2, \quad (1.6)$$

E^2

But calculate gravitational radiation from ultrarelativistic body is hard!

Can we calculate the Self-force?

II. SELF-FORCE IN GENERAL RELATIVITY

The local self-force in 3+1 gravity with zero cosmological constant was derived originally by Mino, Sasaki and Tanaka and also Queen and Wald [2, 3]. As we noted in the introduction and now we repeat for completeness,

$$m\ddot{x}^a = G_5 m^2 \dot{x}^b \dot{x}^c \int_{-\infty}^{\tau_-} d\tau' \qquad (2.1)$$
$$\left(\frac{1}{2}\nabla^a \mathbf{G}^-_{bca'b'} - \nabla_b \mathbf{G}^{-\,a}_{c\ \ a'b'} - \frac{1}{2}\dot{x}^a\dot{x}^d\nabla_d\,\mathbf{G}^-_{bca'b'}\right)\dot{x'}^a\dot{x'}^b,$$

But does it actually work? It is zero in flat 3+1 dimensions!

2+1 matches exactly the radiation

Self-force

$$2+1: \quad (m\ddot{x}^a)_L \approx -\frac{2e^2}{\sqrt{3}} \frac{\ddot{x}\cdot\ddot{x}}{\sqrt{\ddot{x}\cdot\ddot{x}}}\dot{x}^a,$$

$$4+1: \quad (m\ddot{x}^a)_L \approx -\frac{e^2}{10\sqrt{3}} \frac{\dddot{x}\cdot\dddot{x}}{\sqrt{\ddot{x}\cdot\ddot{x}}}\dot{x}^a,$$

- We calculated it in flat 2+1 and 4+1 dimensions
- Grav.self-force in thermal (B.H.) AdS5 calculated in 2 frames, lab and ``the hot wind" one

$$m\ddot{x}^a \approx -\frac{G_5 m^2}{30\pi}\left(\frac{4}{\sqrt{6\,\dddot{x}\cdot\dddot{x}}}\right)\mathbf{R}^m{}_e{}^n{}_b\mathbf{R}_{mcnd}\,\dot{x}^e\dot{x}^b\dot{x}^c\dot{x}^d\,\dot{x}^a,$$

$$f_{self} \sim \gamma^2 m^2/N_c^2$$

$$f_{string} \sim \sqrt{\lambda}\gamma T^2$$

m,n=5, but a,b,c,d,e are ||

$m^2 gamma^2 => E^2$ as in 1973

Subleading in Nc
but may be large …

II. SELF-FORCE IN GENERAL RELATIVITY

The local self-force in 3+1 gravity with zero cosmological constant was derived originally by Mino, Sasaki and Tanaka and also Queen and Wald [2, 3]. As we noted in the introduction and now we repeat for completeness,

$$m\ddot{x}^a = G_5 m^2 \dot{x}^b \dot{x}^c \int_{-\infty}^{\tau_-} d\tau' \left(\frac{1}{2}\nabla^a \mathbf{G}^-_{bca'b'} - \nabla_b \mathbf{G}^{-a}_{\ c\ a'b'} - \frac{1}{2}\dot{x}^a \dot{x}^d \nabla_d \mathbf{G}^-_{bca'b'}\right) \dot{x'}^a \dot{x'}^b, \tag{2.1}$$

with $\mathbf{G}^-$ being the graviton retarded propagator,

$$\Box \mathbf{G}^-_{aba'b'} - 2\,\mathbf{R}^c{}_{ab}{}^d\,\mathbf{G}^-_{cda'b'} = -16\pi\,\overline{g}_{aa'}\overline{g}_{bb'}\,\delta_5(x,x'), \tag{2.2}$$

where $x = x(\tau)$, $x' = x(\tau')$, $\delta_5(x,x') = \delta^5(x-x')\sqrt{-g}$ and $\overline{g}$ is DeWitt's bilocal for parallel displacement along the geodesic [18]. Although the original derivation of (2.1) was carried in 3+1 dimensional space with zero cosmological constant and matter, its physical interpretation is applicable in any dimensions: the right-hand side is simply a modification of Christoffel symbols due to the retarded metric perturbation of the particle trajectory. Therefore we assume it to hold in general, especially for thermal AdS_5 in 4+1 dimensions.

For ultrarelativistic jets, the eikonal limit is appropriate

$$\mathbf{G}^-_{aba'b'}(x,x') \approx 16\pi\,\overline{g}_{aa'}\,\overline{g}_{bb'}\,\mathbf{G}^-(x,x'), \tag{2.3}$$

with $\Box \mathbf{G}^-(x,x') = -\delta_5(x,x')$. Inserting (2.3) in (2.1) yields

$$m\dot{x}^a \approx 4\pi^2\,G_5\,m^2 \int_{-\infty}^{\tau_-} d\tau' \left((\nabla^a \mathbf{G}^- - \dot{x}^a \dot{x}^d \nabla_d \mathbf{G}^-)(\dot{x}\cdot\dot{x'})^2 - 2\,\dot{x}\cdot\dot{x'}\dot{x'}^a \dot{x}^d \nabla_d \mathbf{G}^-\right). \tag{2.4}$$

In the above, we have dropped terms of the type $\nabla^a \overline{g}$ as they are subleading in small proper time ϵ-expansion than $\nabla^a \mathbf{G}^-$.

The scalar retarded propagator in a curved background of 4+1 dimensions can be related to the one in 2+1 dimensions. Explicitly,

$$\mathbf{G}^-(x,x') = -\frac{1}{2\pi}\frac{d}{d\sigma}\left(\Theta(x',x)\frac{\theta(-\sigma)}{2\pi}\frac{\sqrt{\Delta}}{\sqrt{-2\sigma}}\right), \tag{2.5}$$

where the expression inside the bracket is the retarded propagator in 2+1 dimensions. $\Theta(x',x)$ is the generalized heaviside step-function with a space-like surface through x (the final form (2.5) doesn't depend on the choice of this surface), and Δ is the Van-Vleck determinant

$$\Delta(x,x') = (g(x)g(x'))^{1/2}\,\det\left(\nabla_a \nabla_{a'}\sigma(x,x')\right), \tag{2.6}$$

which is a scalar two-point function. σ is an another two-point scalar function

$$\sigma(x,x') = \frac{1}{2}(\tau-\tau')\int_{\tau'}^{\tau} d\tau''\,\dot{x}(\tau'')\cdot\dot{x}(\tau''), \tag{2.7}$$

which is defined by the geodesic between x and x'. It is negative for time-like geodesics

$$\sigma(x,x') = -\frac{1}{2}(\tau-\tau')^2 = \frac{1}{2}d(x,x')^2, \tag{2.8}$$

where $d(x,x')$ is the chordal distance. While the latter is only defined locally for general curved space-times, it can be defined globally for dS and AdS spaces because of their spherical and hyperbolic nature. Indeed, for AdS_5 the finite distance is

$$\cos\left(d(x,x')\right) - 1 = \frac{(\mathbf{x}-\mathbf{x}')^2}{2zz'}, \tag{2.9}$$

with z being the conformal direction and $\mathbf{x}^2 = -t^2 + x^2$. This relation is readily derived by embedding AdS_5 in R^6 with a hyperbolic constraint. We further note that the retarded propagator in AdS_5 is the known function of (2.5) derived in [19], and our generic small time expansion is consistent with it.

III. SELF-FORCE ON JETS IN ADS$_5$

A. The expansion in ϵ

For ultrarelativistic jets, the trajectory is characterized by small proper times, and one can expand in it. Inserting (2.5) into (2.4) and following our arguments for the self-force in 4+1 dimensions show that the gravitational self-force for ultrarelativistic jets is dominated by the leading singularity in the (covariant) gradient of the propagator,

$$\nabla^a \mathbf{G}^- \approx -\frac{3}{4\pi^2}\frac{\sqrt{\Delta}\,\sigma^a}{\epsilon^5}, \tag{3.1}$$

with small $\epsilon = (\tau-\tau') \ll 1$. The smallness of ϵ will be explained further below. The problem is then reduced to a covariant expansion of $\sqrt{\Delta}$ for x' near x. For that we follow [18, 20] and expand $\sqrt{\Delta}$ first covariantly in terms of the world function σ and then proceed to Taylor expand σ. Specifically

$$\sqrt{\Delta} = 1 + \frac{1}{12}\mathbf{R}_{ab}\,\sigma^a\sigma^b - \frac{1}{24}\mathbf{R}_{ab;c}\,\sigma^a\sigma^b\sigma^c + \left(\frac{1}{288}\mathbf{R}_{ab}\mathbf{R}_{cd} + \frac{1}{360}\mathbf{R}^m{}_a{}^n{}_b\mathbf{R}_{mcnd} + \frac{1}{60}\mathbf{R}_{ab;cd}\right) \times\sigma^a\sigma^b\sigma^c\sigma^d + \cdots, \tag{3.2}$$

For both empty and thermal AdS spaces there are significant simplifications, which come from the fact that

$$\sigma|_{\rm flat} \approx -\frac{\epsilon^2}{2} - \frac{\epsilon^4}{12}\,\ddot{x}\cdot\ddot{x} \tag{3.9}$$

For ultrarelativistic motion, we can make the substitution

$$\epsilon \to \epsilon\left(1 + \frac{1}{6}\,\epsilon^2\,\ddot{x}\cdot\ddot{x}\right)^{1/2} \tag{3.10}$$

leading to a finite resummed result

$$\int_0^\infty d\epsilon\,\left(1 + \frac{1}{6}\epsilon^2\,\ddot{x}\cdot\ddot{x}\right)^{-5/2} = \frac{4}{\sqrt{6\,\ddot{x}\cdot\ddot{x}}} \tag{3.11}$$

with most of the contribution stemming from the range $\epsilon \approx 1/\gamma^2$. As a result, the dropped terms in our quasi-local analysis of the gravitational self-force are all subleading in $1/\gamma$. This argument shows how a schematic resummation of the subleading corrections yields a finite result for $\int d\epsilon$. The qualitative character of this subtitution does not fix the overall coefficient exactly. For that, more quantitative work is needed.

Summary

- **ALICE&LHC: 30% larger elliptic (and radial) flows, exactly as Hydro 1 predicted already 10 years ago! => QGP @ LHC remains a very good liquid !**
- **Hydro 2: Quantitative analytic theory in the linear approximation => Green function for Gubser flow) reproduces the correlators beautifully, best with viscosity** $\frac{4\pi\eta}{\hbar s} \approx 2$
- **Falling membrane and 2 types of observables: nonlocal see equilibration in more detail. 5-dim echo effect!**
- **Entropy and trapped surface: jump in multiplcity?**
- **Large energy deposition to matter from jets: Perhaps a longitudinal braking force**
- **Self-force of gravitaitonal nature? O(E^2) ?**

extras

Concentric circles in WMAP data may provide evidence of violent pre-Big-Bang activity

By V. G. Gurzadyan[1] and R. Penrose[2]

1.Yerevan Physics Institute and Yerevan State University, Yerevan, 0036, Armenia
2. Mathematical Institute,24-29 St Giles', Oxford OX1 3LB, U.K.

Note: not 1° but few times larger!

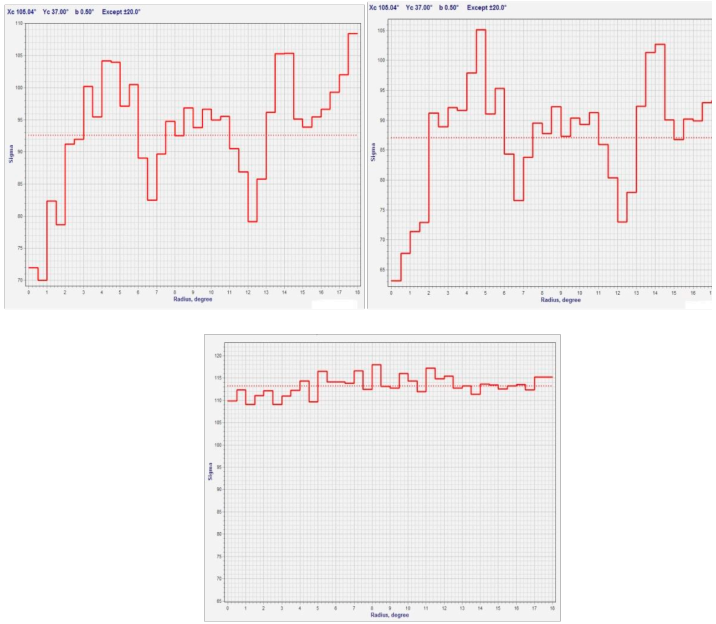

Figure 2. The temperature variance ring structures in WMAP W (a) and V (b) band maps. The Gaussian map simulated for WMAP W parameters is shown as well (c).

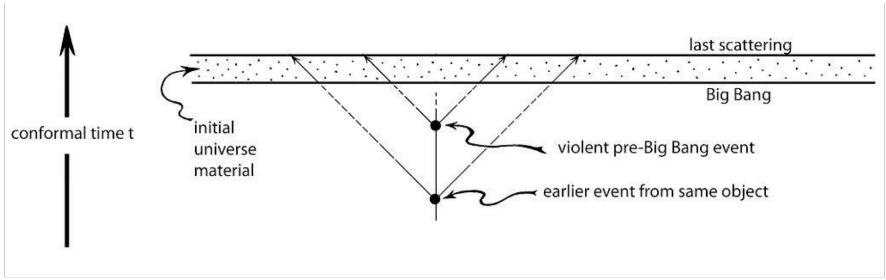

Figure 1.Conformal diagram (without inflation) according to CCC, where a pre-Big-Bang object (presumably a galactic cluster containing supermassive black-holes) is the source of two violent events.

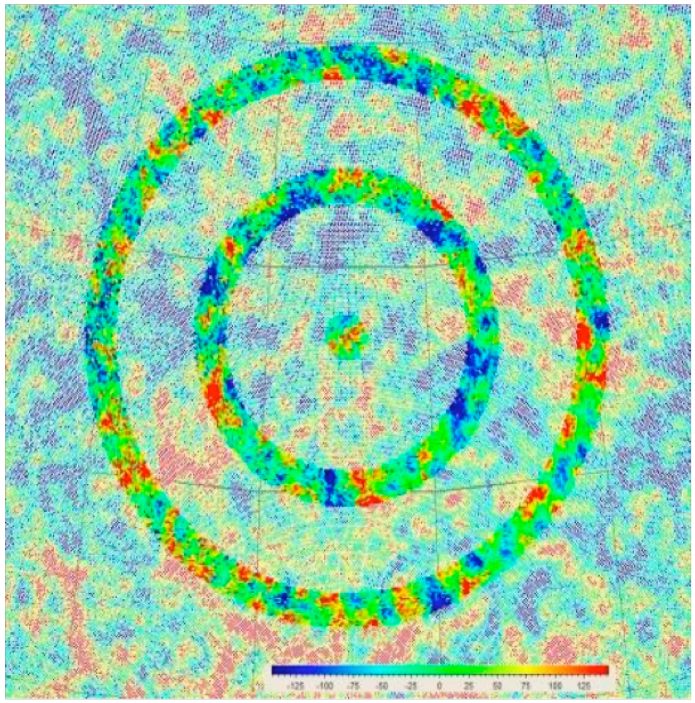

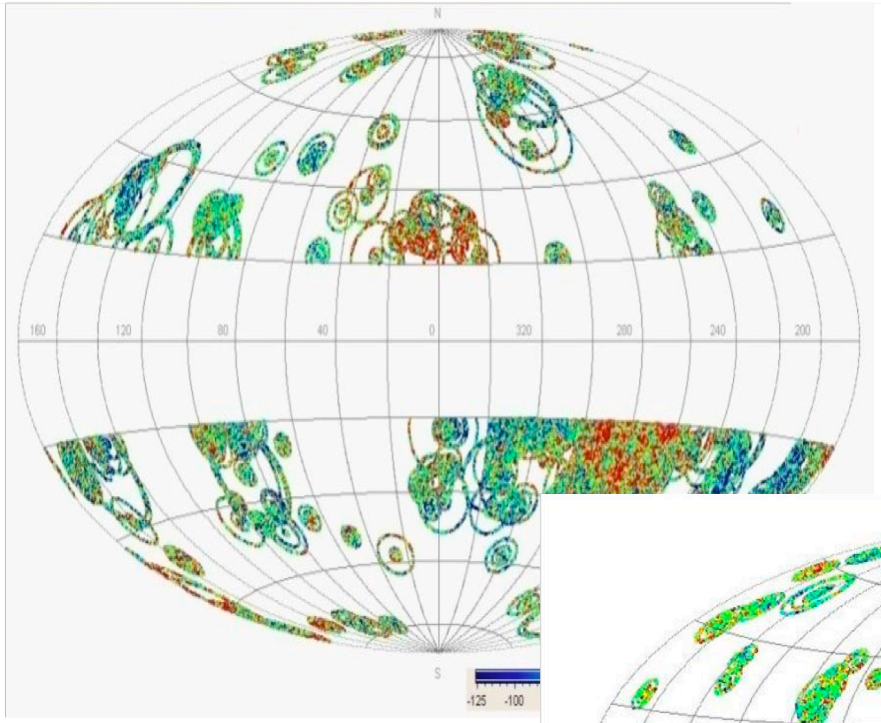

e 4. The sky distribution of concentric sets containing three
ates the positions of the centres, the lower one exhibits the actu

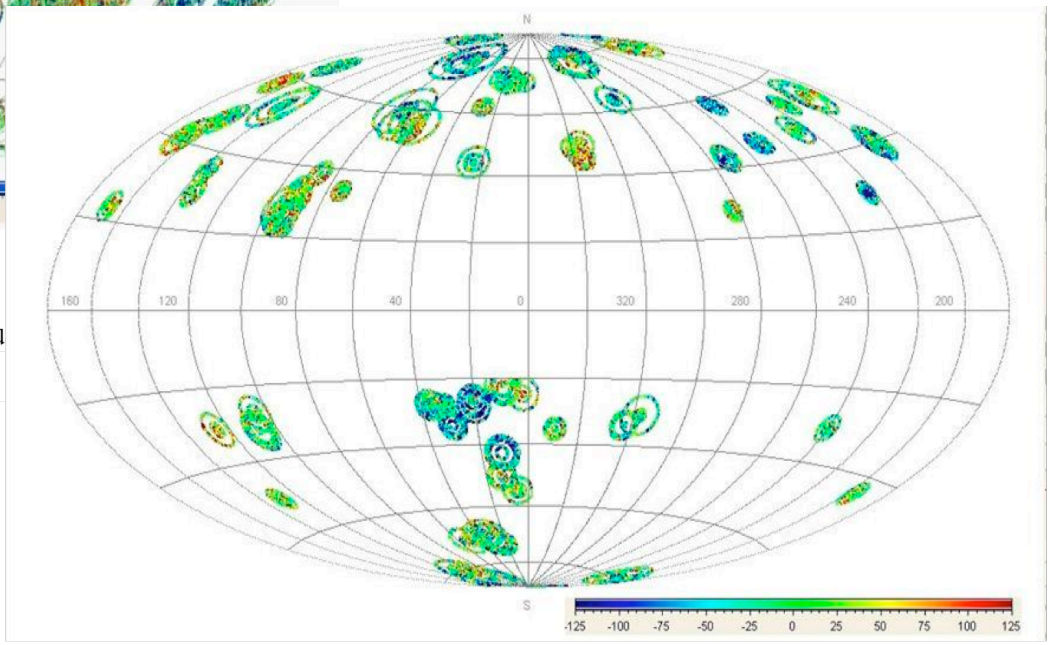

Figure 5. The corresponding maps to those of Figure 4, but where a simulated CMB sky is used incorporating WMAP's *l*-spectrum with randomized *m*-values. The differences are striking, notably the many fewer concentric sets, the absence of significant inhomogeneities and of large circles, and the much smaller departures from the average CMB temperatures.

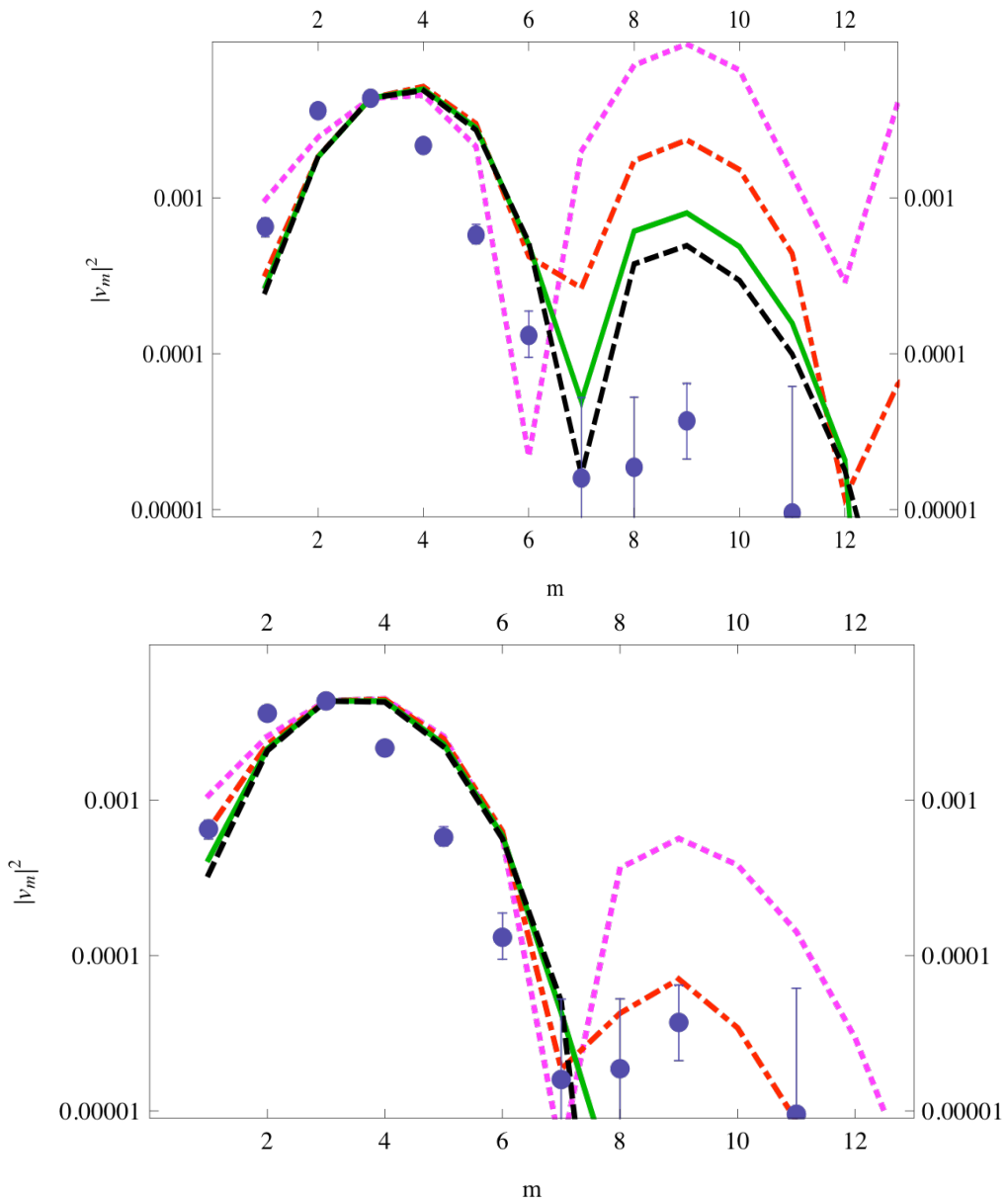

The power spectrum

Points – ATLAS preliminary

upper plot: small size perturbation, various viscosities
Lower plot: about 1 fm size

A dip around m=7 and maximum around 9 have The same acoustic origin as in the Big Bang => zero amplitude of the ``observable combination" at freezeout